tamyl transpeptidase (γ-GTP), albumin (ALB), and total protein (TP) in rAAV2-α-SG- and rAAV8-α-SG-injected Sgca$^{-/-}$ mice. Because skeletal muscle contains isozymes of creatine kinase, lactate dehydrogenase, aspartate aminotransferase, and ALT, these may be released into the blood stream after muscle necrosis (Janssen *et al.*, 1989); the ALT level in Sgca$^{-/-}$ mice was 5.4-fold higher than that in Sgca$^{+/+}$ mice ($p < 0.001$; Table 1). The ALT level in rAAV8-injected Sgca$^{-/-}$ mice was slightly lower than that in Sgca$^{-/-}$ mice. The levels of other liver-related proteins, including γ-GTP, ALB, and TP, were not significantly different between Sgca$^{-/-}$ and rAAV2-α-SG- and rAAV8-α-SG-injected Sgca$^{-/-}$ mice.

Tropism of rAAV2- and rAAV8-α-SG in α-SG-deficient mice

To investigate whether there is any difference in tissue tropism between rAAV2 and rAAV8, we determined the vector copies per diploid genome (C/DG) between the two vectors in injected skeletal muscle by a quantitative, real-time PCR assay. We injected neonatal Sgca$^{-/-}$ mice with either rAAV2-α-SG or rAAV8-α-SG at three different doses (1×10^{10}, 5×10^{10}, or 1×10^{11} VG/mouse) via the TA muscle ($n = 3$ per group). At a dose of 1×10^{11} VG/mouse, we detected rAAV2-α-SG and rAAV8-α-SG vector genomes in skeletal muscle at levels of 0.05 ± 0.03 and 5.33 ± 1.88 C/DG, respectively ($p < 0.01$; Fig. 3A). Increasing doses of rAAV8-α-SG resulted in increased levels of transgene expression. Higher transduction efficiency was observed with rAAV8-α-SG when large amounts of vector were used. Moreover, to evaluate the amount of α-SG in rAAV2-α-SG- or rAAV8-α-SG-injected skeletal muscles of Sgca$^{-/-}$ mice, we performed Western blot analysis. Four weeks after injection of rAAV2-α-SG into the TA muscle of neonatal and adult Sgca$^{-/-}$ mice, α-SG was almost undetectable (Fig. 3B). In contrast, when rAAV8-α-SG was injected into the right TA muscle of neonatal Sgca$^{-/-}$ mice, the amount of α-SG in rAAV8-transduced muscles was 3.5-fold higher than that in Sgca$^{+/+}$ muscles. When transduced in adulthood, the expression level of α-SG in the TA muscle of Sgca$^{-/-}$ mice was almost equal to that in Sgca$^{+/+}$ muscle. In addition, α-SG was detected in contralateral hind limb muscles and the heart after injection of rAAV8-α-SG into the TA muscle (Fig. 3B).

rAAV8-mediated α-SG expression ameliorated muscle pathology

A defect in any one of the four SGs can disrupt the entire SG complex in LGMD 2C-2F patients. Thus, we investigated the presence of a SG complex in the sarcolemma 4 weeks after injection of rAAV8-α-SG into the TA muscle of neonatal Sgca$^{-/-}$ mice. Immunostaining of rAAV8-α-SG-injected TA muscle with anti-SGs antibodies revealed that restoration of α-SG expression accompanied the sarcolemmal expression of other components of the SG complex, that is, β-, γ-, and δ-SG (Fig. 4). Moreover, 4 weeks after rAAV8-α-SG injection, H&E staining demonstrated considerable amelioration of the muscle pathology of rAAV8-injected TA muscles (Fig. 5A), and of surrounding EDL, SOL, GAS, and TP/PL muscles (data not shown). In contrast, uninjected and rAAV2-α-SG-injected muscles of Sgca$^{-/-}$ mice still showed signs of muscle degeneration and regeneration. To evaluate the amelioration of the dystrophic phenotype (Morgan *et al.*, 1990; Duclos *et al.*, 1998; Li *et al.*, 1999; Allamand *et al.*, 2000; Dressman *et al.*, 2002), we counted centrally nucleated myofibers in rAAV8-α-SG-injected muscles 4 months after injection (Fig. 5B). Sgca$^{-/-}$ hind limb muscles showed approximately 90% centrally nucleated myofibers. In contrast, rAAV8-α-SG-injected TA and ipsilateral EDL and SOL muscles showed

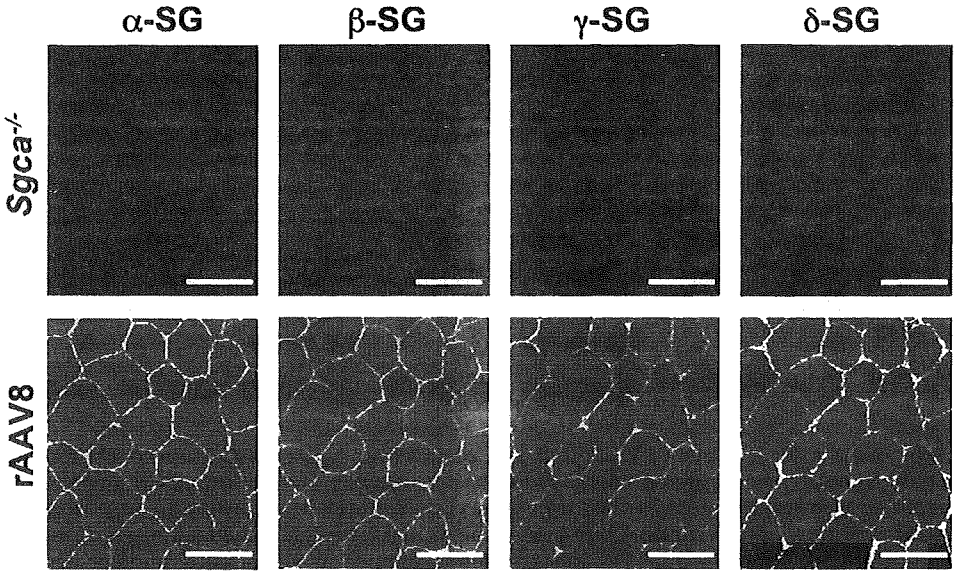

FIG. 4. Complete restoration of sarcoglycan expression at the sarcolemma of α-SG-deficient muscle after rAAV8-α-SG injection. Right TA muscles of neonatal Sgca$^{-/-}$ mice were injected with 1×10^{11} VG of rAAV8-α-SG. Untreated and rAAV8-injected Sgca$^{-/-}$ TA muscles (*top* and *bottom*, respectively) were labeled by indirect immunofluorescence, using specific antibodies against β-SG, γ-SG, or δ-SG. Untreated Sgca$^{-/-}$ muscle showed a secondary loss of SGs from the sarcolemma. Four weeks after injection, SGs were expressed in rAAV8-injected Sgca$^{-/-}$ muscle. Scale bars: 50 μm.

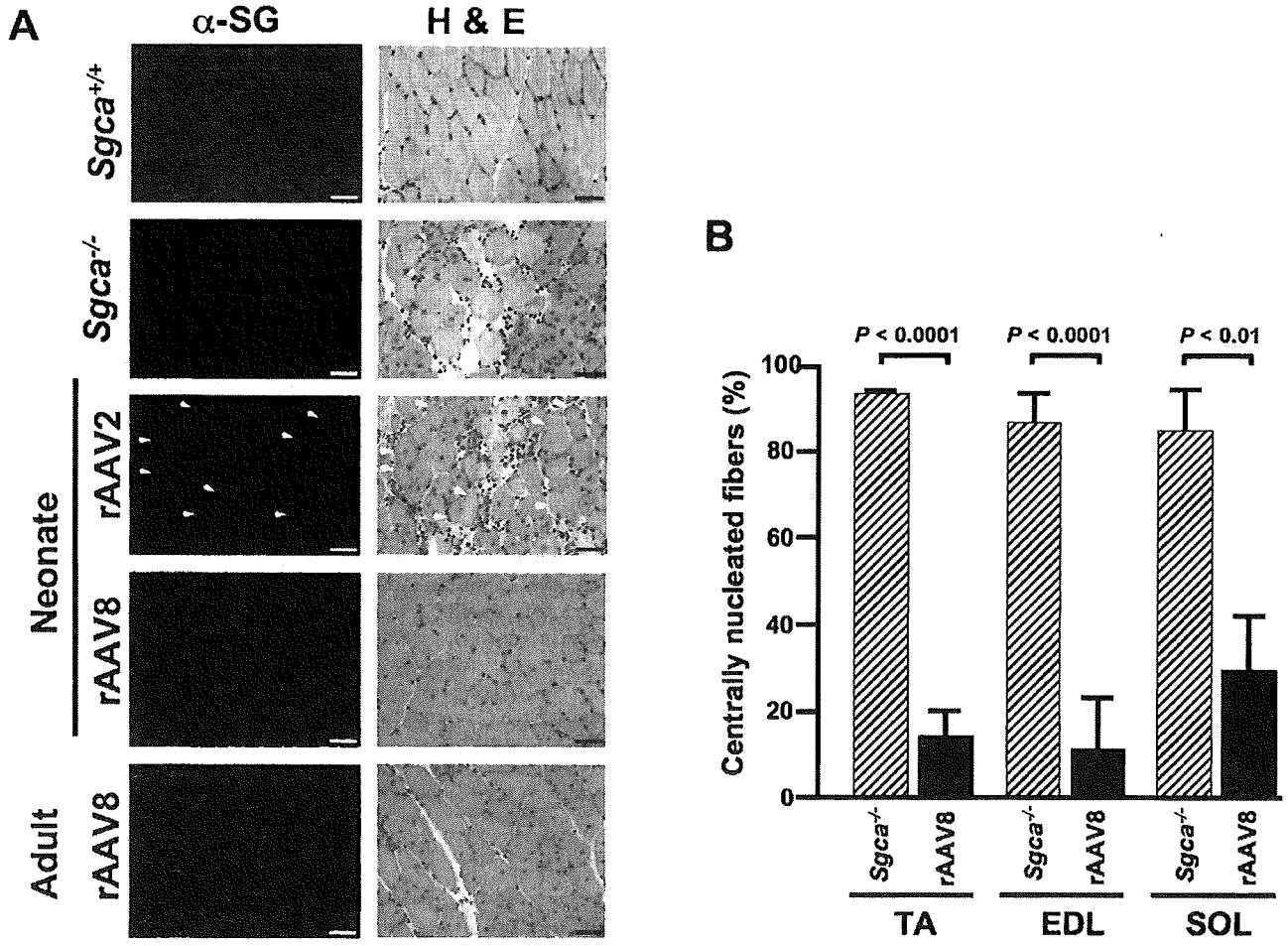

FIG. 5. Reduction of muscle degeneration in α-SG-deficient mice after rAAV8-α-SG-mediated gene transfer. (**A**) Right TA muscles of neonatal or adult Sgca $^{-/-}$ mice were transduced with 1×10^{11} VG (neonates) or 5×10^{11} VG (adults) of rAAV2-α-SG or rAAV8-α-SG. Four weeks after rAAV injection, serial cross-sections of Sgca $^{+/+}$, Sgca $^{-/-}$, and rAAV2- or rAAV8-injected Sgca $^{-/-}$ TA muscles (rAAV2 and rAAV8, respectively) were labeled by indirect immunofluorescence, using α-SG antibody (*left*, green), and stained with hematoxylin and eosin (H&E) (*right*). rAAV8-injected Sgca $^{-/-}$ TA muscles showed no signs of muscle degeneration. Arrowheads indicate α-SG-positive fibers. Scale bars: 50 μm. (**B**) Percentages of centrally nucleated myofibers in Sgca $^{-/-}$ skeletal muscles 4 months after injection of rAAV8-α-SG. Right TA muscles of neonatal Sgca $^{-/-}$ mice were transduced with 1×10^{11} VG of rAAV8-α-SG. Centrally nucleated myofibers among more than 200 total myofibers were counted in randomly selected H&E-stained cross-sections of the hind limb from Sgca $^{-/-}$ mice (hatched columns) and rAAV8-α-SG-injected Sgca $^{-/-}$ mice (solid columns) ($n = 3$ for each group). The percentage of centrally nucleated myofibers in rAAV8-α-SG-injected Sgca $^{-/-}$ mice was significantly lower than that in untreated Sgca $^{-/-}$ mice. p Values showed a statistically significant difference between Sgca $^{-/-}$ mice and rAAV8-injected Sgca $^{-/-}$ mice ($p < 0.0001$ for TA, $p < 0.0001$ for EDL, and $p < 0.01$ for SOL).

13.2 ± 7.3, 10.4 ± 10.4, and 29.1 ± 12.9% centrally nucleated myofibers, respectively ($p < 0.0001$, $p < 0.0001$, and $p < 0.0023$, respectively; Fig. 5B). The percentage of centrally nucleated myofibers in rAAV8-injected hind limb was significantly lower than that of Sgca $^{-/-}$ muscle, indicating that full recovery of the SG complex at the sarcolemma of Sgca $^{-/-}$ mice corrected the underlying biochemical deficiency and consequently restored the integrity of the muscle membrane.

rAAV-8-mediated α-SG expression improves contractile force and reverses muscle hypertrophy of α-SG-deficient muscle

A major functional deficit in muscular dystrophy patients is the loss of muscle strength. In our previous physiological study of muscular dystrophy model animals, we confirmed profound muscle force deficits in TA muscle (Yoshimura *et al.*, 2004; Imamura *et al.*, 2005).

A deficiency of α-SG decreases the contractile force of affected muscles (Danieli-Betto *et al.*, 2005; Imamura *et al.*, 2005). To evaluate whether rAAV8-α-SG transfer might improve Sgca $^{-/-}$ muscle physiological function, we measured the contractile force of rAAV8-injected Sgca $^{-/-}$ TA and EDL muscles. TA and EDL muscles were carefully separated from the hind limb and subjected to *in vitro* electrophysiological stimulation and contractile measurement on a force transducer. First, the right TA muscles of neonatal Sgca $^{-/-}$ mice were transduced with 1×10^{11} VG of rAAV8-α-SG. At the age of 5 months, the specific tetanic force of untreated Sgca $^{+/+}$ and Sgca $^{-/-}$ TA muscles was 17.3 ± 4.5 and 8.9 ±

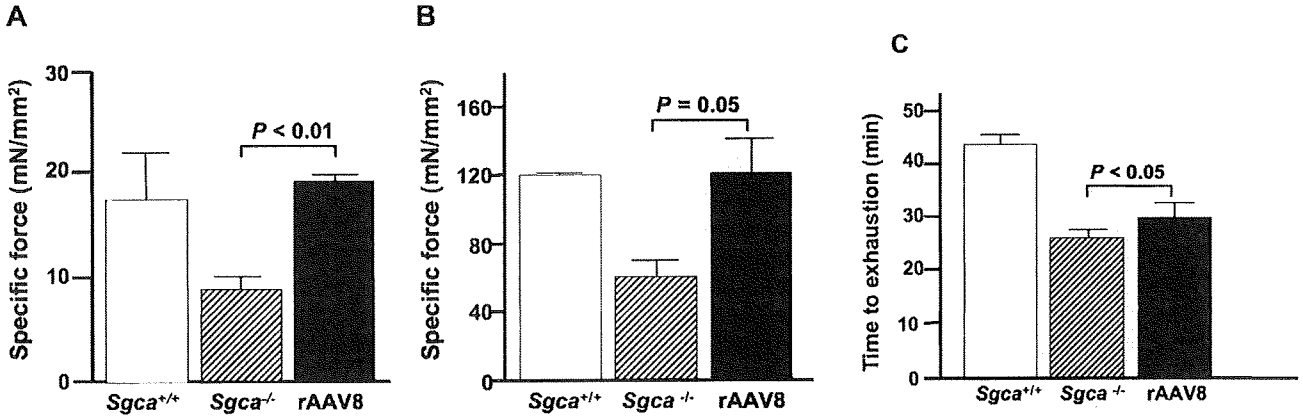

FIG. 6. Recovery of contractile force of α-SG-deficient muscle after transduction with rAAV8-α-SG. Right TA muscles of neonatal or adult Sgca$^{-/-}$ mice were transduced with 1×10^{11} VG (neonates) or 5×10^{11} VG (adults) of rAAV8-α-SG, and tetanic forces and time to exhaustion were assessed *in vitro* and *in vivo*. (**A**) Specific tetanic force of TA muscles from Sgca$^{+/+}$ (open column, $n = 3$), untreated Sgca$^{-/-}$ (hatched column, $n = 3$), and rAAV8-α-SG-injected Sgca$^{-/-}$ mice (solid column, $n = 3$). The right TA muscles of neonatal Sgca$^{-/-}$ mice were transduced with 1×10^{11} VG of rAAV8-α-SG, and the tetanic forces of TA muscles were assessed *in vitro* 5 months after injection. (**B**) Specific tetanic force of EDL muscles from Sgca$^{+/+}$ (open column, $n = 3$), untreated Sgca$^{-/-}$ (hatched column, $n = 3$), and rAAV8-α-SG-injected Sgca$^{-/-}$ mice (solid column, $n = 4$). The right TA muscles of adult Sgca$^{-/-}$ mice were transduced with 5×10^{11} VG of rAAV8-α-SG, and the tetanic forces of EDL muscles were assessed *in vitro* 10 weeks after injection. The p values show a statistically significant difference between Sgca$^{-/-}$ mice and rAAV8-injected Sgca$^{-/-}$ mice ($p < 0.01$ for TA, and $p = 0.05$ for EDL). (**C**) Time to exhaustion in treadmill test: Sgca$^{+/+}$ (open column, $n = 3$), untreated Sgca$^{-/-}$ (hatched column, $n = 4$), and rAAV8-α-SG-injected Sgca$^{-/-}$ mice (solid column, $n = 4$). The right TA muscles of adult Sgca$^{-/-}$ mice were transduced with 5×10^{11} VG of rAAV8-α-SG, and the tetanic forces of EDL muscles were assessed *in vitro* 10 weeks after injection. The p values show a statistically significant difference between Sgca$^{-/-}$ mice and rAAV8-injected Sgca$^{-/-}$ mice ($p < 0.05$).

1.2 mN/mm^2, respectively, whereas that of rAAV8-injected Sgca$^{-/-}$ TA muscle was 19.4 ± 0.7 mN/mm^2 ($p < 0.01$; Fig. 6A and Table 2). Furthermore, we assessed the improvement of EDL muscle after rAAV8-α-SG injection in adulthood. rAAV8-α-SG (5×10^{11} VG) was injected into the right TA muscle of adult Sgca$^{-/-}$ mice. We measured the contractile force of the EDL muscle surrounding rAAV8-injected TA muscle 10 weeks after injection. The specific tetanic forces of Sgca$^{+/+}$ and Sgca$^{-/-}$ EDL muscles were 121.5 ± 1.6 and 61.74 ± 8.33 mN/mm^2, and that of rAAV8-injected Sgca$^{-/-}$ EDL muscle was 121.15 ± 22.12 mN/mm^2 ($p = 0.05$; Fig. 6B and Table 2). Consequently, the specific tetanic force of animals injected with rAAV8-α-SG was 2-fold higher than that of uninjected Sgca$^{-/-}$ TA muscle ($p < 0.01$, and $p = 0.05$; Fig. 6A and B, Table 2).

In addition to the drastic improvement in contractile force of rAAV8-α-SG-injected TA muscle, the weight of rAAV8-α-SG-injected TA and EDL muscles as a percentage of body weight was comparable to those of Sgca$^{+/+}$ muscle and much smaller than those of their untreated counterparts (Table 2), suggesting that rAAV8-α-SG treatment reduced the muscle hypertrophy of Sgca$^{-/-}$ muscle. Moreover, we investigated whether α-SG expression in Sgca$^{-/-}$ muscle effectively increases the physical performance of the muscle. In an enforced treadmill test, the exhaustion times of Sgca$^{-/-}$ and rAAV8-α-SG injected Sgca$^{-/-}$ mice were 25.9 ± 2.0 and 30 ± 2.6 min ($p < 0.05$; Fig. 6C). rAAV8-injected Sgca$^{-/-}$ mice demonstrated increased exercise time before reaching exhaustion and could run longer distances.

Discussion

In this paper, we have presented evidence that a single intramuscular injection of a rAAV8 vector expressing human α-SG cDNA via a CMV promoter could achieve efficient therapeutic effects in a dystrophic animal model of LGMD 2D.

When rAAV8-α-SG was administered to neonatal Sgac$^{-/-}$ mice, we observed extensive α-SG transduction in the hind limb muscles, including the TA, EDL, SOL, and GAS muscles. In the case of rAAV8 injection of adult Sgac$^{-/-}$ mice, α-SG was expressed not only in all of the hind limb muscles and but also in cardiac muscle. A similar profile was further confirmed in a study by Wang and coworkers, in which they delivered more potent double-stranded rAAV8 vectors into adult and neonatal mice. The rAAV8 vector is more stable in the bloodstream than other rAAV serotypes when administered intravascularly and extravascularly (Wang *et al.*, 2005). The 37/67-kDa laminin receptor (LamR) has been identified as the host cell receptor for the AAV8 vector (Akache *et al.*, 2006). LamR is widely expressed in human tissues, where it is normally involved in interactions of extracellular laminin-1 with proteases and the cell (Ardini *et al.*, 1997, 2002). Furthermore, the rAAV8 vector might be able to cross the capillary endothelial cell barrier and transduce remote organs with high efficiency (Inagaki *et al.*, 2006). However, the detailed mechanism of rAAV8-mediated cell recognition and transduction has yet to be fully elucidated.

In the present study, we demonstrated that rAAV8-α-SG transduced skeletal muscle about 100-fold more compared with rAAV2-α-SG. In addition, rAAV8-α-SG-injected

TABLE 2. CONTRACTILE PROPERTIES OF rAAV8-INJECTED α-SARCOGLYCAN DEFICIENT MUSCLE[a,b]

	Injection age	*Number of mice*	*Tissue*	*Muscle length* (L_o, *mm*)	*Muscle weight* (*mg*)	*Tissue weight* (*% of body weight*)	*CSA* (mm^2)	*Maximal contraction* (P_o, *mN*)	*Specific force* (mN/mm^2)
$Sgca^{+/+}$	10-day-old	3	TA	11	56.1 ± 2.9	0.185 ± 0.004	4.81 ± 0.14	82.3 ± 19.2	17.3 ± 4.5
$Sgca^{-/-}$	10-day-old	3	TA	11.5	68.1 ± 6.9	0.233 ± 0.023	5.61 ± 0.32	48.5 ± 4.0	8.9 ± 1.2
rAAV8-injected $Sgca^{-/-}$	10-day-old	3	TA	11.5	65.7 ± 8.2	0.224 ± 0.027	5.05 ± 0.46	103.8 ± 10.3	19.4 ± 0.7[c]
$Sgca^{+/+}$	7-week-old	3	EDL	14.83 ± 0.83	11.30 ± 0.46	0.044 ± 0.001	0.73 ± 0.07	88.3 ± 8.5	121.5 ± 1.6
$Sgca^{-/-}$	7-week-old	3	EDL	14	13.5 ± 0.48	0.047 ± 0.002	0.91 ± 0.03	56.94 ± 9.25	61.74 ± 8.33
rAAV8-Injected $Sgca^{-/-}$	7-week-old	4	EDL	14	10.7 ± 0.84	0.038 ± 0.003	0.72 ± 0.06[d]	84.04 ± 8.74	121.15 ± 22.12[e]

Abbreviations: CSA, tissue cross-sectional area; EDL, extensor digitorum longus; TA, tibialis anterior.

[a]Data represent means ± SE. Tissue weights were normalized to respective body weights.

[b]The *p* values indicate statistical significance between $Sgca^{-/-}$ mice and rAAV8-injected $Sgca^{-/-}$ mice.

[c]$p < 0.01$ when rAAV8 was injected into neonatal $Sgca^{-/-}$ TA muscle.

[d]$p \leq 0.05$ when rAAV8 was injected into adult $Sgca^{-/-}$ EDL muscle.

[e]$p \leq 0.05$ when rAAV8 was injected into adult $Sgca^{-/-}$ EDL muscle.

Sgca $^{-/-}$ mice did not demonstrate cytotoxic and immunological reactions for more than 7 months after injection. Transduction of α-SG in an LGMD 2D animal model by means of adenovirus, rAAV1, or rAAV2 vector was previously reported (Duclos *et al.*, 1998; Allamand *et al.*, 2000; Dressman *et al.*, 2002; Fougerousse *et al.*, 2007; Pacak *et al.*, 2007). In the two studies using the adenovirus vector, it was necessary to use neonatal animals to take advantage of the immaturity of the immune system and thereby to circumvent the strong immune response elicited by the adenoviral vector (Duclos *et al.*, 1998; Allamand *et al.*, 2000). The AAV vector, which has been more widely used, is nonpathogenic, has low immunogenicity, and has been shown to confer long-term gene expression in muscles of various species. Use of the ubiquitous CMV promoter would allow expression of the transgene in various cells. Therefore, expression of α-SG via rAAV1 and rAAV2, using the CMV promoter, induced an immune response, whereas those vectors introduced balanced expression of SGs within the injected Sgca$^{-/-}$ myofibers (Duclos *et al.*, 1998; Allamand *et al.*, 2000; Dressman *et al.*, 2002; Fougerousse *et al.*, 2007; Pacak *et al.*, 2007). Between 28 and 41 days after rAAV2 injection, a drastic decrease in α-SG expression occurred in the injected Sgca$^{-/-}$ muscle. In particular, numerous antigen-presenting cells in the dystrophic muscles could direct a strong immune response against the transgene product when the CMV promoter was used (Yuasa *et al.*, 2002). On the other hand, the AAV8 vector transduced antigen-presenting cells (such as dendritic cells) less efficiently than did the rAAV2 vector (Xin *et al.*, 2006). Consequently, gene transduction via the AAV2 vector with the CMV promoter might be less efficient than with rAAV8 and other AAV serotypes.

Because the CMV promoter elicits an immune response against the transgene product (Cordier *et al.*, 2001; Yuasa *et al.*, 2002; Liu *et al.*, 2004), several studies of rAAV-mediated transduction of striated musculature used the muscle creatine kinase (MCK), CK6, or SP6 promoter as a muscle-specific promoter (Gregorevic *et al.*, 2004; Yoshimura *et al.*, 2004; Zhu *et al.*, 2005). Transduction driven by a muscle-specific promoter was achieved without acute toxicological response. Moreover, to enable strong expression in striated muscle, another group created a hybrid promoter containing the MCK enhancer and the simian virus 40 promoter (MCK/SV40 promoter) (Takeshita *et al.*, 2007). The MCK/SV40 promoter yielded long-term (>6 months) expression of a human secretory alkaline phosphatase (huSEAP) reporter gene after electrotransfer of the plasmid into mice. In addition, selection of the rAAV serotype is important. rAAV9 has also been shown to be efficient in cardiac or skeletal muscle transduction (Inagaki *et al.*, 2006; Sarkar *et al.*, 2006).

Our study demonstrated improvement of the contractile force and decreased sensitivity to stretch and exhaustion time for exercise in Sgca$^{-/-}$ muscle after rAAV8-α-SG injection. Recovery of absolute maximal force and specific tetanic force is one of the barometers of amelioration. A dose of about 1×10^{11} VG (for neonates) or 5×10^{11} VG (for adults) in Sgca$^{-/-}$ TA muscle led to transduction of approximately >70% of hind limb muscles and was sufficient to increase the global force of the animal. We compared tetanic contractions of rAAV8-α-SG-injected muscles with those of Sgca$^{+/+}$ and Sgca$^{-/-}$ muscles. The contractile forces of rAAV8-injected Sgca$^{-/-}$ TA and EDL muscles were increased 2-fold compared with that of Sgca $^{-/-}$ muscles. Furthermore, the exercise treadmill test results for rAAV8-injected Sgca$^{-/-}$ mice were higher than those of Sgca $^{-/-}$ mice. This suggested that increased synthesis of α-SG had no adverse effects on SG complex formation, and that overexpression of α-SG might induce stability of the transmembrane without causing muscle pathology. In a therapeutic study using rAAV1 (Fougerousse *et al.*, 2007), injection of rAAV1 encoding α-SG cDNA via the C5-12 promoter (a muscle-specific promoter) into the artery of Sgca $^{-/-}$ mice increased the contractile force of EDL muscles 1.5-fold compared with that of Sgca$^{-/-}$ EDL muscles. Therefore, rAAV8 would be an effective tool for the delivery of therapeutic genes to skeletal muscles in the treatment of limb-girdle muscular dystrophy.

Acknowledgments

The authors greatly appreciate the technical support and helpful discussion provided by Ms. Kazue Kinoshita and Dr. Katsutoshi Yuasa. We thank Dr. Eva Engvall for providing the Sgca $^{-/-}$ mice. This work was supported by a Grant for Research on Nervous and Mental Disorders (16B-2) and by Health Science Research Grants for Research on the Human Genome and Gene Therapy (H16-genome-003) and for Research on Brain Science (H15-kokoro-021 and H18-kokoro-019) from the Ministry of Health, Labor, and Welfare; and by Grants in Aid for Scientific Research (16390418, 16590333, 18590392, and 19390383) from the Ministry of Education, Culture, Sports, Science, and Technology.

References

Akache, B., Grimm, D., Pandey, K., Yant, S.R., Xu, H., and Kay, M.A. (2006). The 37/67-kilodalton laminin receptor is a receptor for adeno-associated virus serotypes 8, 2, 3, and 9. J. Virol. 80, 9831–9836.

Allamand, V., Donahue, K.M., Straub, V., Davisson, R.L., Davidson, B.L., and Campbell, K.P. (2000). Early adenovirus-mediated gene transfer effectively prevents muscular dystrophy in α-sarcoglycan-deficient mice. Gene Ther. 7, 1385–1391.

Araishi, K., Sasaoka, T., Imamura, M., Noguchi, S., Hama, H., Wakabayashi, E., Yoshida, M., Hori, T., and Ozawa, E. (1999). Loss of the sarcoglycan complex and sarcospan leads to muscular dystrophy in β-sarcoglycan-deficient mice. Hum. Mol. Genet. 8, 1589–1598.

Ardini, E., Tagliabue, E., Magnifico, A., Buto, S., Castronovo, V., Colnaghi, M.I., and Menard, S. (1997). Co-regulation and physical association of the 67-kDa monomeric laminin receptor and the $\alpha_6\beta_4$ integrin. J. Biol. Chem. 272, 2342–2345.

Ardini, E., Sporchia, B., Pollegioni, L., Modugno, M., Ghirelli, C., Castiglioni, F., Tagliabue, E., and Menard, S. (2002). Identification of a novel function for 67-kDa laminin receptor: Increase in laminin degradation rate and release of motility fragments. Cancer Res. 62, 1321–1325.

Bonnemann, C.G., Modi, R., Noguchi, S., Mizuno, Y., Yoshida, M., Gussoni, E., McNally, E.M., Duggan, D.J., Angelini, C., and Hoffman, E.P. (1995). β-Sarcoglycan (A3b) mutations cause autosomal recessive muscular dystrophy with loss of the sarcoglycan complex. Nat. Genet. 11, 266–273.

Burton, M., Nakai, H., Colosi, P., Cunningham, J., Mitchell, R., and Couto, L. (1999). Coexpression of factor VIII heavy and light chain adeno-associated viral vectors produces biologically active protein. Proc. Natl. Acad. Sci. U.S.A. 96, 12725–12730.

Cordier, L., Gao, G.P., Hack, A.A., McNally, E.M., Wilson, J.M., Chirmule, N., and Sweeney, H.L. (2001). Muscle-specific promoters may be necessary for adeno-associated virus-mediated gene transfer in the treatment of muscular dystrophies. Hum. Gene Ther. 12, 205–215.

Danieli-Betto, D., Esposito, A., Germinario, E., Sandona, D., Martinello, T., Jakubiec-Puka, A., Biral, D., and Betto, R. (2005). Deficiency of α-sarcoglycan differently affects fast- and slow-twitch skeletal muscles. Am. J. Physiol. Regul. Integr. Comp. Physiol. 289, R1328–R1337.

Dressman, D., Araishi, K., Imamura, M., Sasaoka, T., Liu, L.A., Engvall, E., and Hoffman, E.P. (2002). Delivery of α- and β-sarcoglycan by recombinant adeno-associated virus: Efficient rescue of muscle, but differential toxicity. Hum. Gene Ther. 13, 1631–1646.

Duclos, F., Straub, V., Moore, S.A., Venzke, D.P., Hrstka, R.F., Crosbie, R.H., Durbeej, M., Lebakken, C.S., Ettinger, A.J., Van Der Meulen, J., Holt, K.H., Lim, L.E., Sanes, J.R., Davidson, B.L., Faulkner, J.A., Williamson, R., and Campbell, K.P. (1998). Progressive muscular dystrophy in α-sarcoglycan-deficient mice. J. Cell Biol. 142, 1461–1471.

Ervasti, J.M., Ohlendieck, K., Kahl, S.D., Gaver, M.G., and Campbell, K.P. (1990). Deficiency of a glycoprotein component of the dystrophin complex in dystrophic muscle. Nature 345, 315–319.

Eymard, B., Romero, N.B., Leturcq, F., Piccolo, F., Carrie, A., Jeanpierre, M., Collin, H., Deburgrave, N., Azibi, K., Chaouch, M., Merlini, L., Themar-Noel, C., Penisson, I., Mayer, M., Tanguy, O., Campbell, K.P., Kaplan, J.C., Tome, F.M., and Fardeau, M. (1997). Primary adhalinopathy (α-sarcoglycanopathy): Clinical, pathologic, and genetic correlation in 20 patients with autosomal recessive muscular dystrophy. Neurology 48, 1227–1234.

Fanin, M., Duggan, D.J., Mostacciuolo, M.L., Martinello, F., Freda, M.P., Soraru, G., Trevisan, C.P., Hoffman, E.P., and Angelini, C. (1997). Genetic epidemiology of muscular dystrophies resulting from sarcoglycan gene mutations. J. Med. Genet. 34, 973–977.

Fisher, K.J., Jooss, K., Alston, J., Yang, Y., Haecker, S.E., High, K., Pathak, R., Raper, S.E., and Wilson, J.M. (1997). Recombinant adeno-associated virus for muscle directed gene therapy. Nat. Med. 3, 306–312.

Fougerousse, F., Bartoli, M., Poupiot, J., Arandel, L., Durand, M., Guerchet, N., Gicquel, E., Danos, O., and Richard, I. (2007). Phenotypic correction of α-sarcoglycan deficiency by intra-arterial injection of a muscle-specific serotype 1 rAAV vector. Mol. Ther. 15, 53–61.

Gao, G., Vandenberghe, L.H., Alvira, M.R., Lu, Y., Calcedo, R., Zhou, X., and Wilson, J.M. (2004). Clades of adeno-associated viruses are widely disseminated in human tissues. J. Virol. 78, 6381–6388.

Gao, G.P., Alvira, M.R., Wang, L., Calcedo, R., Johnston, J., and Wilson, J.M. (2002). Novel adeno-associated viruses from rhesus monkeys as vectors for human gene therapy. Proc. Natl. Acad. Sci. U.S.A. 99, 11854–11859.

Greelish, J.P., SU, L.T., Lankford, E.B., Burkman, J.M., Chen, H., Konig, S.K., Mercier, I.M., Desjardins, P.R., Mitchell, M.A., Zheng, X.G., Leferovich, J., Gao, G.P., Balice-Gordon, R.J., Wilson, J.M., and Stedman, H.H. (1999). Stable restoration of the sarcoglycan complex in dystrophic muscle perfused with histamine and a recombinant adeno-associated viral vector. Nat. Med. 5, 439–443.

Gregorevic, P., Blankinship, M.J., Allen, J.M., Crawford, R.W., Meuse, L., Miller, D.G., Russell, D.W., and Chamberlain, J.S. (2004). Systemic delivery of genes to striated muscles using adeno-associated viral vectors. Nat. Med. 10, 828–834.

Imamura, M., Araishi, K., Noguchi, S., and Ozawa, E. (2000). A sarcoglycan–dystroglycan complex anchors Dp116 and utrophin in the peripheral nervous system. Hum. Mol. Genet. 9, 3091–3100.

Imamura, M., Mochizuki, Y., Engvall, E., and Takeda, S. (2005). ε-Sarcoglycan compensates for lack of α-sarcoglycan in a mouse model of limb-girdle muscular dystrophy. Hum. Mol. Genet. 14, 775–783.

Inagaki, K., Fuess, S., Storm, T.A., Gibson, G.A., McTiernan, C.F., Kay, M.A., Nakai, H., Sarkar, R., Mucci, M., Addya, S., Tetreault, R., Bellinger, D.A., Nichols, T.C., and Kazazian, H.H., Jr. (2006). Robust systemic transduction with AAV9 vectors in mice: Efficient global cardiac gene transfer superior to that of AAV8. Mol. Ther. 14, 45–53.

Iwata, Y., Nakamura, H., Mizuno, Y., Yoshida, M., Ozawa, E., and Shigekawa, M. (1993). Defective association of dystrophin with sarcolemmal glycoproteins in the cardiomyopathic hamster heart. FEBS Lett. 329, 227–231.

Janssen, G.M., Kuipers, H., Willems, G.M., Does, R.J., Janssen, M.P., and Geurten, P. (1989). Plasma activity of muscle enzymes: Quantification of skeletal muscle damage and relationship with metabolic variables. Int. J. Sports Med. 10(Suppl. 3), S160–S168.

Kessler, P.D., Podsakoff, G.M., Chen, X., McQuiston, S.A., Colosi, P.C., Matelis, L.A., Kurtzman, G.J., and Byrne, B.J. (1996). Gene delivery to skeletal muscle results in sustained expression and systemic delivery of a therapeutic protein. Proc. Natl. Acad. Sci. U.S.A. 93, 14082–14087.

Kyhse-Andersen, J. (1984). Electroblotting of multiple gels: A simple apparatus without buffer tank for rapid transfer of proteins from polyacrylamide to nitrocellulose. J. Biochem. Biophys. Methods 10, 203–209.

Laemmli, U.K. (1970). Cleavage of structural proteins during the assembly of the head of bacteriophage T4. Nature 227, 680–685.

Li, J., Dressman, D., Tsao, Y.P., Sakamoto, A., Hoffman, E.P., and Xiao, X. (1999). rAAV vector-mediated sarcoglycan gene transfer in a hamster model for limb girdle muscular dystrophy. Gene Ther. 6, 74–82.

Liu, Y.L., Mingozzi, F., Rodriguez-Colon, S.M., Joseph, S., Dobrzynski, E., Suzuki, T., High, K.A., and Herzog, R.W. (2004). Therapeutic levels of factor IX expression using a muscle-specific promoter and adeno-associated virus serotype 1 vector. Hum. Gene Ther. 15, 783–792.

McNally, E.M., Yoshida, M., Mizuno, Y., Ozawa, E., and Kunkel, L.M. (1994). Human adhalin is alternatively spliced and the gene is located on chromosome 17q21. Proc. Natl. Acad. Sci. U.S.A. 91, 9690–9694.

Morgan, J.E., Hoffman, E.P., and Partridge, T.A. (1990). Normal myogenic cells from newborn mice restore normal histology to degenerating muscles of the *mdx* mouse. J. Cell Biol. 111, 2437–2449.

Mourkioti, F., Kratsios, P., Luedde, T., Song, Y.H., Delafontaine, P., Adami, R., Parente, V., Bottinelli, R., Pasparakis, M., and Rosenthal, N. (2006). Targeted ablation of IKK2 improves skeletal muscle strength, maintains mass, and promotes regeneration. J. Clin. Invest. 116, 2945–2954.

Nigro, V., De Sa Moreira, E., Piluso, G., Vainzof, M., Belsito, A., Politano, L., Puca, A.A., Passos-Bueno, M.R., and Zatz, M. (1996). Autosomal recessive limb-girdle muscular dystrophy, LGMD2F, is caused by a mutation in the δ-sarcoglycan gene. Nat. Genet. 14, 195–198.

Noguchi, S., McNally, E.M., Ben Othmane, K., Hagiwara, Y., Mizuno, Y., Yoshida, M., Yamamoto, H., Bonnemann, C.G., Gussoni, E., Denton, P.H., Kyriakides, T., Middleton, L., Hen-

tati, F., Ben Hamida, M., Nonaka, I., Vance, J.M., Kunkel, L.M., and Ozawa, E. (1995). Mutations in the dystrophin-associated protein γ-sarcoglycan in chromosome 13 muscular dystrophy. Science 270, 819–822.

Noguchi, S., Wakabayashi, E., Imamura, M., Yoshida, M., and Ozawa, E. (1999). Developmental expression of sarcoglycan gene products in cultured myocytes. Biochem. Biophys. Res. Commun. 262, 88–93.

Pacak, C.A., Walter, G.A., Gaidosh, G., Bryant, N., Lewis, M.A., Germain, S., Mah, C.S., Campbell, K.P., and Byrne, B.J. (2007). Long-term skeletal muscle protection after gene transfer in a mouse model of LGMD-2D. Mol. Ther. 15, 1775–1781.

Sarkar, R., Mucci, M., Addya, S., Tetreault, R., Bellinger, D.A., Nichols, T.C., and Kazazian, H.H., Jr. (2006). Long-term efficacy of adeno-associated virus serotypes 8 and 9 in hemophilia a dogs and mice. Hum. Gene Ther. 17, 427–439.

Takeshita, F., Takase, K., Tozuka, M., Saha, S., Okuda, K., Ishii, N., and Sasaki, S. (2007). Muscle creatine kinase/SV40 hybrid promoter for muscle-targeted long-term transgene expression. Int. J. Mol. Med. 19, 309–315.

Wang, Z., Zhu, T., Qiao, C., Zhou, L., Wang, B., Zhang, J., Chen, C., Li, J., and Xiao, X. (2005). Adeno-associated virus serotype 8 efficiently delivers genes to muscle and heart. Nat. Biotechnol. 23, 321–328.

Wigler, M., Perucho, M., Kurtz, D., Dana, S., Pellicer, A., Axel, R., and Silverstein, S. (1980). Transformation of mammalian cells with an amplifiable dominant-acting gene. Proc. Natl. Acad. Sci. U.S.A. 77, 3567–3570.

Xiao, X., Li, J., and Samulski, R.J. (1996). Efficient long-term gene transfer into muscle tissue of immunocompetent mice by adeno-associated virus vector. J. Virol. 70, 8098–8108.

Xiao, X., Li, J., and Samulski, R.J. (1998). Production of high-titer recombinant adeno-associated virus vectors in the absence of helper adenovirus. J. Virol. 72, 2224–2232.

Xiao, X., Li, J., Tsao, Y.P., Dressman, D., Hoffman, E.P., and Watchko, J.F. (2000). Full functional rescue of a complete muscle (TA) in dystrophic hamsters by adeno-associated virus vector-directed gene therapy. J. Virol. 74, 1436–1442.

Xin, K.Q., Mizukami, H., Urabe, M., Toda, Y., Shinoda, K., Yoshida, A., Oomura, K., Kojima, Y., Ichino, M., Klinman, D., Ozawa, K., and Okuda, K. (2006). Induction of robust immune responses against human immunodeficiency virus is supported by the inherent tropism of adeno-associated virus type 5 for dendritic cells. J. Virol. 80, 11899–11910.

Yamamoto, H., Mizuno, Y., Hayashi, K., Nonaka, I., Yoshida, M., and Ozawa, E. (1994). Expression of dystrophin-associated protein 35DAG (A4) and 50DAG (A2) is confined to striated muscles. J. Biochem. 115, 162–167.

Yoshida, M., and Ozawa, E. (1990). Glycoprotein complex anchoring dystrophin to sarcolemma. J. Biochem. 108, 748–752.

Yoshimura, M., Sakamoto, M., Ikemoto, M., Mochizuki, Y., Yuasa, K., Miyagoe-Suzuki, Y., and Takeda, S. (2004). AAV vector-mediated microdystrophin expression in a relatively small percentage of *mdx* myofibers improved the *mdx* phenotype. Mol. Ther. 10, 821–828.

Yuasa, K., Sakamoto, M., Miyagoe-Suzuki, Y., Tanouchi, A., Yamamoto, H., Li, J., Chamberlain, J.S., Xiao, X., and Takeda, S. (2002). Adeno-associated virus vector-mediated gene transfer into dystrophin-deficient skeletal muscles evokes enhanced immune response against the transgene product. Gene Ther. 9, 1576–1588.

Zhu, T., Zhou, L., Mori, S., Wang, Z., McTiernan, C.F., Qiao, C., Chen, C., Wang, D.W., Li, J., and Xiao, X. (2005). Sustained whole-body functional rescue in congestive heart failure and muscular dystrophy hamsters by systemic gene transfer. Circulation 112, 2650–2659.

Address reprint requests to:
Dr. Shin'ichi Takeda or Dr. Takashi Okada
Department of Molecular Therapy
National Institute of Neuroscience, NCNP
4-1-1 Ogawa-higashi, Kodaira
Tokyo 187-8502, Japan

E-mail: takeda@ncnp.go.jp or t-okada@ncnp.go.jp

Received for publication January 4, 2008; accepted after revision May 14, 2008.

Published online: June 17, 2008.

Available online at www.sciencedirect.com
ScienceDirect
Journal of Clinical Neuroscience 15 (2008) 757–763
Journal of Clinical Neuroscience
www.elsevier.com/locate/jocn

Clinical Study

Follow-up of three patients with a large in-frame deletion of exons 45–55 in the Duchenne muscular dystrophy (*DMD*) gene

Akinori Nakamura [a,b,*], Kunihiro Yoshida [a], Kazuhiro Fukushima [a], Hideho Ueda [c], Nobuyuki Urasawa [b], Jun Koyama [d], Yoshikazu Yazaki [d], Masahide Yazaki [a], Toshiaki Sakai [e], Seiichi Haruta [f], Shin'ichi Takeda [b], Shu-ichi Ikeda [a]

[a] *Department of Neurology, Shinshu University School of Medicine, Matsumoto 390-8621, Japan*
[b] *Department of Molecular Therapy, National Institute of Neuroscience, NCNP, Kodaira, Japan*
[c] *Department of Anatomy and Cell Biology, School of Health Sciences, Shinshu University, Matsumoto, Japan*
[d] *Department of Cardiology, Shinshu University School of Medicine, Matsumoto, Japan*
[e] *Division of Neurology, Nagano Matsushiro General Hospital, Matsushiro, Nagano, Japan*
[f] *Cardiology Division, Fukuyama Cardiovascular Hospital, Fukuyama, Japan*

Received 21 September 2006; accepted 22 December 2006

Abstract

We review the clinical status of skeletal involvement and cardiac function in three unrelated patients harboring an in-frame deletion of exons 45 to 55 in the *DMD* gene followed up for 2 to 7 years. Two younger patients diagnosed as having X-linked dilated cardiomyopathy (XLDCM) developed congestive heart failure without overt skeletal myopathy. Heart failure recurred after viral infection but responded well to diuretics and angiotensin-converting enzyme inhibitors. One older patient diagnosed with Becker muscular dystrophy showed limb-girdle muscular atrophy and weakness at the age of 50, but did not have any cardiac symptoms. Skeletal muscle involvement in each patient remained unchanged, and cardiac function did not worsen in any of the patients during the study. In a younger XLDCM patient, the amount and molecular weight of mutant dystrophin were equally slightly decreased in both skeletal and cardiac muscles. Immunostaining for dystrophin and dystrophin-associated proteins was slightly reduced in both skeletal and cardiac muscle, with no discernible difference between the two. The phenotype of this dystrophinopathy can manifest as XLDCM in younger patients; however, careful attention to cardiac management may result in a favorable prognosis.

Keywords: Duchenne muscular dystrophy gene; Dystrophin; Becker muscular dystrophy; X-linked dilated cardiomyopathy, cadiomyopathy; Dystrophin

1. Introduction

Dystrophinopathy is caused by a mutation in the Duchenne muscular dystrophy (*DMD*) gene and includes three clinical phenotypes: Duchenne and Becker muscular dystrophies (DMD/BMD) and X-linked dilated cardiomyopathy (XLDCM). XLDCM was originally reported by Berko and Swift[1] and is characterized by preferential cardiac involvement without overt clinical signs of skeletal myopathy. Some mutations in the *DMD* gene causing XLDCM have been reported,[2–11] and it has been proposed that XLDCM can be divided into two groups: those having mutations in the 5' end of the gene and those with mutations in the spectrin-like regions.[12] One of the mechanisms for XLDCM in patients with mutations in the 5' end of the gene is associated with a difference in expression patterns of dystrophin isoforms between skeletal and cardiac muscle.[4,13–15] Generally, in-frame deletion mutations in the spectrin-like region cause the phenotype of BMD, but some cases have been described as having XLDCM[7,12] or presenting with dilated cardiomyopathy alone.[16,17] The mechanism responsible for XLDCM pathology in those with mutations in the spectrin-like region has not been

* Corresponding author. Tel.: +81 263 37 2673; fax: +81 263 34 3427.
E-mail address: anakamu@ncnp.go.jp (A. Nakamura).

0967-5868/$ - see front matter © 2007 Elsevier Ltd. All rights reserved.
doi:10.1016/j.jocn.2006.12.012

elucidated thus far, but two possibilities are proposed: loss of a protein domain specific for the function of cardiac muscle or loss of intronic transcriptional regulating sequences.[12,18] In general, the prognosis of XLDCM patients having mutations in the 5' end of the gene is poor; however, the clinical course of those with dystrophinopathy caused by mutations in the spectrin-like domain has not been fully described. Here, we report the prognosis of patients harboring a deletion of exons 45–55 in the *DMD* gene that cause an in-frame deletion of the spectrin-like domain and the hinge III region of dystrophin.

We previously reported two patients with a large deletion of exons 45 to 55 in the *DMD* gene suffering from XLDCM[20] or adult-onset BMD.[21] Together with another newly found XLDCM patient with the same deletion, these patients have been followed up for 2–7 years to evaluate changes in skeletal and cardio-myopathies. The skeletal muscle involvement did not progress in either of the younger XLDCM patients. On the other hand, cardiac function in all of the patients worsened following viral infection, although it was pharmacologically reversible. The adult-onset BMD patient was self-sufficient, with no heart failure observed during this study. Thus, the prognosis of this type of dystrophinopathy may not be so poor if proper cardiac management is undertaken.

2. Patients and methods

2.1. Case reports

Patient 1 was a 28-year-old Japanese man whose birth and development was normal. At the age of 26, he was admitted to a hospital because of palpitation, low-grade fever, general fatigue, and dry cough during meals or conversation. Blood examination revealed an elevated serum creatine kinase (CK) level (650 U/L), but other biochemical markers including plasma brain-type natriuretic polypeptide (BNP) which is a useful biomarker of heart failure, were within the normal range. Chest X-ray showed cardiomegaly, and the electrocardiogram (ECG) showed a small q-wave in leads I and aVL. Subsequently, the patient was referred to the cardiology department in our hospital. Echocardiography revealed diffuse hypokinesis of the left ventricular wall and dilation of the left ventricle. His ejection fraction (EF) and fractional shortening (FS) was 0.32 (normal > 0.60) and 17.8% (normal > 28%), respectively. His mother's brothers died of cardiac disease at younger ages, but the mother herself had neither cardiac symptoms nor abnormal findings by blood examination, electrocardiography or echocardiography. Because he had hyper-CKemia, the patient was referred to our department of neurology. Neurologic examination revealed no muscle atrophy or weakness of the extremities and normo- or hyper-reflexia of all deep tendons. No calf muscle hypertrophy or contractures of the ankle joints was observed. Serum creatine kinase (CK) level was elevated to 579 IU/L (normal upper limit 164 IU/L). Upon electromyography (EMG), no short duration or low amplitude potentials were recorded in the proximal muscles. After obtaining informed consent, Southern blotting and multiplex polymerase chain reaction (PCR) using genomic DNA from peripheral leukocytes revealed a deletion of exons 45 to 55 in the *DMD* gene. The patient's clinical status was asymptomatic (0) according to the classification proposed by Beggs et al.[19] He was treated with angiotensin-converting enzyme (ACE) inhibitors, and his cardiac function soon improved. Skeletal muscle involvement has not changed, and cardiac function has remained stable up to his current age of 28.

Patient 2, who has been previously reported,[20] was 42 years old at the time of this study. At the age of 36, he complained of a cough and exertional dyspnea following common cold-like symptoms. His chest X-ray showed cardiomegaly, bilateral pleural effusion, and pulmonary congestion. ECG indicated poor R-wave progression in leads V_1-V_3 and flat T wave in leads I, aVL, V_5 and V_6. Echocardiography showed left ventricular dilation and diffuse hypokinesis of left ventricular wall motion. He was treated with diuretics and ACE inhibitors and recovered completely in a couple of days. His hyper-CKemia level (1347 IU/L) and its dominant MM isoform suggested the presence of skeletal myopathy as a cause of cardiomyopathy, although he had no muscular atrophy, weakness, or calf pseudohypertrophy (clinical status: asymptomatic [0]). At the age of 42, his clinical status (asymptomatic) was unchanged. His serum CK value was still high, but his serum BNP level was within the normal range. His EF and FS on echocardiography findings had improved compared to that at age 36 (Table 1).

Patient 3 was a 76-year-old man, reported to have been diagnosed with adult-onset BMD when he was 69 years old.[21] At the age of 59, he noticed mild limb muscle weakness and difficulty when in a sitting or crouching position, although he continued to work into his 60s. At the age of 69, neurological examination revealed moderate proximal muscular atrophy and weakness and a waddling gait, but he lacked calf pseudohypertrophy. His clinical status was moderate (II), he had experienced no cardiac symptoms, and his serum CK value was 669 IU/L. No left ventricle hypokinesis was observed, and both EF and FS were normal on echocardiography. At the age of 76, walking required effort and muscular atrophy was slightly progressed, but his activities of daily living were unimpaired and he remained independent. His clinical status (moderate [II]) was unchanged, and his serum CK value was 188 IU/L. Although his BNP value was high (66.1 pg/mL; normal range 0–20) and the echocardiography findings revealed a slight hypokinesis of left ventricle wall motion, his EF and FS were still unchanged and he had no cardiac symptoms. In patients 2 and 3, deletion of exons 45–55 in the *DMD* gene was identified by Southern blotting and multiplex PCR (data not shown).[20,21] We have now reviewed the clinical status of skeletal and cardiac involvement in the three patients, both at admission and for this study (Table 1).

Table 1
Summary of clinical course of patients with a large deletion of exons 45–55 in the *DMD* gene

Patient no.	1		2		3	
Age (yrs)	26	28	36	42	69	76
Clinical status	0	0	0	0	II	II
Serum CK level (U/l)	650	589	1,347	1,170	669	188
Cardiac failure	(+)	(−)	(+)	(−)	(−)	(−)
Serum BNP level (pg/ml)	12.0	8.1	53.7	4.6	ND	66.1
CTR (%)	56	46	58	50	53	52
Electrocardiogram findings	Small *q* in I, aVL, V_5 and V_6	Small *q* in I, aVL, V_5 and V_6	Poor *R*-wave progression in V_{1-3}	Poor *R*-wave progression in V_{1-3}	Prominent *R*-wave in V_1	Prominent *R*-wave in V_1
LV hypokinesis	Diffuse	Diffuse	Diffuse	Diffuse	None	Slight
LVDd	60.5	63.3	69.0	60.0	56.0	44.0
LVDs	49.7	43.9	60.0	45.0	38.3	31.3
EF	0.32	0.57	0.25	0.48	0.60	0.56
FS (%)	17.8	30.7	12.0	25.0	32.1	28.9

Clinical status was assessed by a previous report; CK: creatine kinase (normal 180 U/l); BNP: brain-type natriuretic peptide (normal < 5.0 pg/ml); CTR: cardiothoracic ratio (normal < 50%); LV: Left ventricle: Dd: end-diastolic dimension (normal 36–54 mm); Ds: end-systolic dimension (normal 25–38 mm); EF: ejection fraction (normal > 0.60); FS: fractional shortening (normal > 28%).

2.2. Molecular and histochemical studies in patient 1

We obtained informed consent and performed skeletal and cardiac muscle biopsies on patient 1. The specimens were frozen in cooled isopentane and stored at −80 °C until analysis. Total RNA from skeletal muscle of patient 1 was extracted, and cDNA was synthesized. The cDNA was amplified using a forward primer specific to exon 44 (5′-TGGGAACATGCTAAATACAAATGG-3′), and a reverse primer specific to exon 56 (5′-GAGCTTCAATTTC-ACCTT GGAGG-3′). Direct sequencing of the PCR product was performed to confirm the deletion at the cDNA level.

For the biochemical analysis of dystrophin, 100 μg of each muscle extract was separated by SDS-polyacrylamide gel electrophoresis and either transferred onto a polyvinyl difluoride (PVDF) membrane or stained with Coomassie Brilliant Blue (CBB). The membranes were-blocked in Tris-buffered saline containing 0.1% Tween 20 (TBST) and 5% skim milk (w/v) and then incubated with a primary anti-dystrophin antibody (NCL-Dys2; Novocastra Laboratories Ltd., Newcastle upon Tyne, UK) at 4 °C overnight. The membranes were washed in TBST and then incubated with mouse-specific horseradish peroxidase-conjugated secondary antibodies followed by detection with enhanced chemiluminescence.

For histochemical analysis, cryostat sections of 7-μm thickness were prepared and stained with hematoxylin and eosin (H&E). Some sections were dried for 15 min and pre-incubated with PBS containing 5% bovine serum albumin (BSA) and heat-inactivated normal goat serum albumin at pH 7.4. The sections were incubated with primary antibodies for 16 h at 4 °C, then with FITC-labeled secondary antibodies (10 μg/mL) at room temperature for 1 h before washing in PBS containing 5% BSA. The sections were mounted in a glycerol-based medium and assessed under a fluorescence microscope. Primary antibodies were used as follows: dystrophin MANEX1A (provided by Dr. GE Morris; epitope: exon 1, aa1-aa10); MANDYS8 (Sigma, St. Louis, MO, USA; epitope: exons 31–32, aa1431-aa1505); NCL-Dys2 (NCL-Dys 2; Novocastra; epitope: exons 78–79, aa3546-aa 3562); F22.9C5 (ALEXIS Biochemicals, Lausen, Switzerland; epitope exons 37–45, aa1840-aa2266); α-, β-, γ-, and δ-sarcoglycans (SGs), α- and β-dystroglycans (DGs) and dysferlin (Novocastra). For Western blotting and immunohistochemistry analyses, we used skeletal muscle from a patient with dermatomyositis as a control.

3. Results

3.1. Clinical characteristics of the patients during the study

In patients 1 and 2, skeletal muscle involvement was unchanged, but it had progressed slightly during the last 7 years in patient 3. Cardiac function of patient 1 was stable during the last 2 years. Patient 2 developed recurrent heart failure after an infection similar to the common cold, but this could be reversed by appropriate therapy. As of the time of this study, patient 3 had not experienced cardiac symptoms (Table 1).

3.2. Molecular, histopathological, and immnohistochemical analyses in patient 1

We examined the extent of the deletion at the mRNA level in patient 1 to confirm the mutation suggested by Southern blot analysis. cDNA from skeletal muscle tissue showed that exon 44 was linked directly to exon 56 in the transcript (Fig. 1B). Based on the genomic DNA and

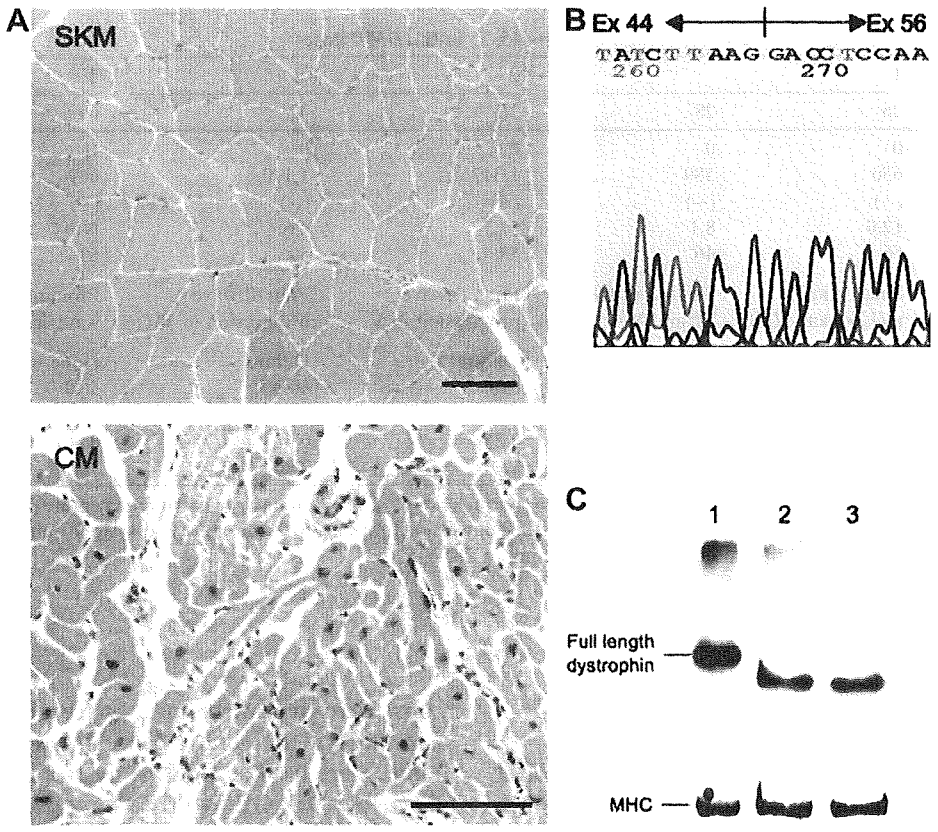

Fig. 1. Histopathological and molecular analyses of patient 1. A: Hematoxylin and eosin (H&E) staining of skeletal (SKM) and cardiac muscles (CM). In skeletal muscle there were slight variations in the sizes of muscle fibers and an increase in the number of fibers with internal nuclei, but proliferation of interstitial connective tissue was not observed. In cardiac muscle, there was slight proliferation of connective tissue, but disarrangement of cardiac fibers was not seen. (Bar = 100 μm) B: Sequencing of the Duchenne muscular dystrophy (DMD) cDNA derived from skeletal muscle. Direct sequencing of the cDNA from patient 1 revealed that exon 44 directly linked to exon 56. C: Western blot analysis of skeletal and cardiac muscles. Lane 1: skeletal muscle of a control patient; lane 2: skeletal muscle of patient 1; lane 3: cardiac muscle of patient 1. As an internal control, myosin heavy chain (MHC) was detected by Coomassie Brilliant Blue staining. The amount and molecular weight of mutant dystrophin were slightly, but equally, decreased as compared to normal skeletal muscle.

cDNA sequences of the *DMD* gene, this mutation was an in-frame deletion, and the predicted molecular weight of mutant dystrophin was about 360 kDa (approximately 15% smaller than the 427 kDa full-length dystrophin). Western blotting analysis using anti-dystrophin antibody showed that the amount and molecular weight of mutant dystrophin were slightly reduced to the same extent in both skeletal and cardiac muscle (Fig. 1C).

H&E staining of skeletal muscle from patient 1 showed a variation in fiber size and hypercontracted fibers, but no necrotic fibers or proliferation of interstitial connective tissue. Cardiac muscle showed a slight proliferation of connective tissue, but disarrangement of cardiac fibers was not observed (Fig. 1A).

Staining of skeletal and cardiac muscles with the anti-dystrophin antibodies MANEX1A (Fig. 2B, a–c), MANDYS8 (Fig. 2B, d–f) and Dys2 (Fig. 2B, j–l) was normal or slightly decreased. However, staining with an antibody against the predicted deleted region of dystrophin (F22.9C5) (Fig. 3B, g–i) was absent at the sarcolemma in both types of muscle in patient 1. Staining with α-DG (Fig. 3A–C), β-DG (Fig. 3D–F), α-SG (Fig. 3G–I) and β-SG (Fig. 3J–L) was slightly reduced in skeletal and cardiac sarcolemma, but the staining patterns were not different between the two types of muscle. There was no difference in staining for γ- and δ-SGs or dysferlin between the two (data not shown).

4. Discussion

We report three patients with dystrophinopathy harboring the same in-frame deletion of exons 45–55 in the *DMD* gene. Generally the phenotype associated with this mutation is predicted to be a milder form because the deletion is in-frame. Some BMD patients with the same deletion mutation have been reported, but the clinical profile in each patient was not addressed.[18,22] The clinical manifestations in the two younger patients studied here (patients 1 and 2) were quite similar: absence of skeletal muscle symptoms despite hyper-CKemia and an episode of heart failure following viral infection. However, it remains possible that they will develop skeletal myopathy in the future, as for patient 3. Although the younger patients are tentatively considered as having XLDCM, cardiac dysfunction was ameliorated by ACE inhibitors and did not progress until

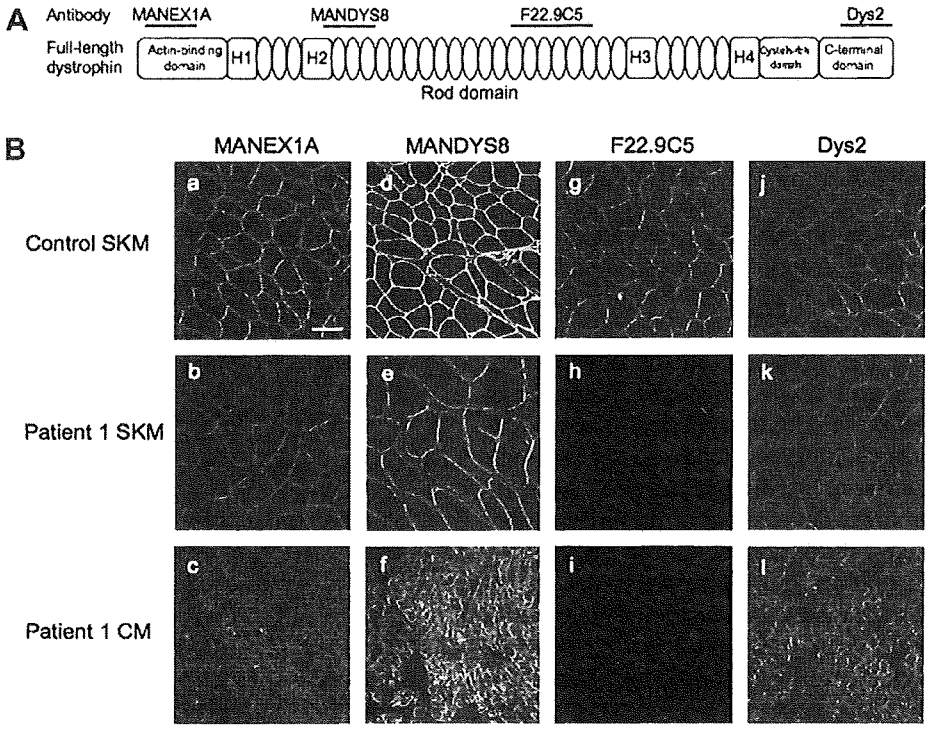

Fig. 2. Expression of dystrophin in skeletal and cardiac muscles from patient 1. A: Anti-dystrophin MANEX1a, NCL-DYSB, F22.9C5, and NCL-DYS2 antibodies recognize different epitopes of dystrophin (see Methods). B: Immunohistochemistry of dystrophin in biopsied skeletal and cardiac muscles. Immunohistochemical analysis using four anti-dystrophin antibodies, MANEX1A (a-c), MANDYS8 (d–f), F22.9C5 (g–i) and Dys2 (j–l), in the biopsied skeletal muscle (SKM) from a control patient (a, d, g and j), skeletal muscle (SKM) from patient 1 (b, e, h and k) and cardiac muscle (CM) from patient 1 (c, f, i and l). Immunoreactivities for MANEX1A, MANDYS8, and Dys 2 were slightly reduced in skeletal and cardiac sarcolemma compared to control skeletal muscle, while no immunoreactivity for F22.9C5, which stains the deleted region in dystrophin, was observed in the patient's muscles. (Bar = 50 μm).

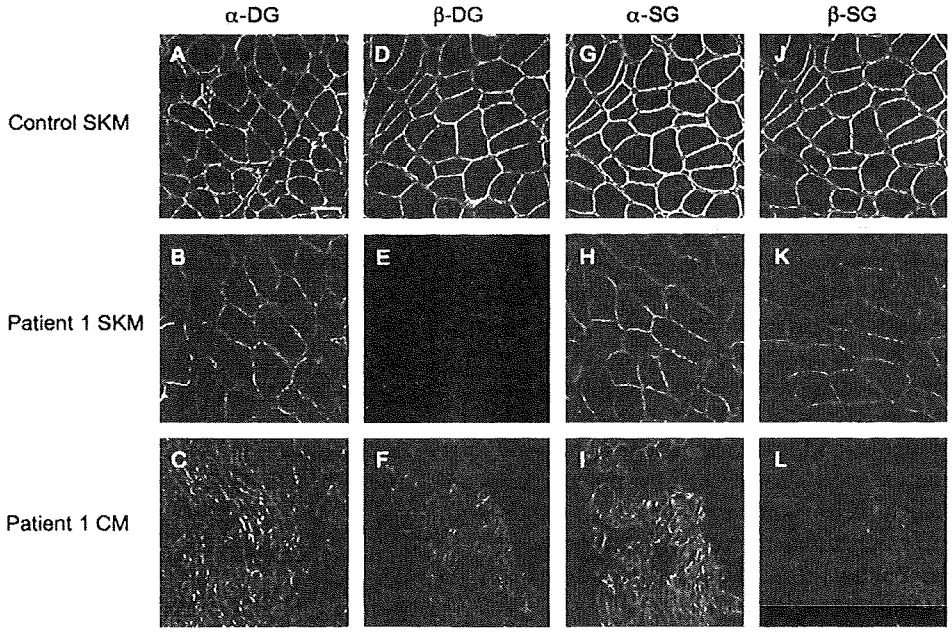

Fig. 3. Expression of dystroglycans and sarcoglycans in skeletal and cardiac muscles from patient 1. Immunohistochemical analyses using antibodies to α-dystroglycan (α-DG) (A–C), β-dystroglycan (β-DG) (D–F), α-sarcoglycan (α-SG) (G–I) and β-sarcoglycan (β-SG) (J– L) in the skeletal muscle (SKM) from a control patient (A, D, G and J) and the skeletal muscle (SKM) (B, E, H and K) and cardiac muscle (CM) (C, F, I and L) from patient 1. Immunoreactivities for α-DG, β-DG, α-SG and β-SG were slightly reduced in the patient's skeletal and cardiac sarcolemma, but the patterns were not different between the two muscles. (Bar = 50 μm).

recently. In current model therapy for DMD cardiomyopathy, early diagnosis and treatment by ACE inhibitors and/or beta-blockers has been recommended to improve cardiac function and symptoms of congestive heart failure[23] and to lead to ventricular remodeling.[24]

What is the mechanism of cardiac dysfunction in the two younger patients? It has been proposed that XLDCM patients with a mutation in the spectrin-like regions of the *DMD* gene may have lost a protein domain specific for the function of cardiac muscle or may have lost intronic transcriptional regulating sequences.[12,18] Non-genetic factors might also account for the differences in the phenotypes. Based upon patients 1 and 2, viral infection might be a trigger for progression of cardiac dysfunction. Those with dystrophin deficiency have been reported to be very susceptible to enterovirus-induced cardiomyopathy.[25] Accordingly, viral infections might have a role in the progression of cardiac disturbances. With respect to the prevention of, or therapy for, heart failure, it is important to determine whether and how viral infection is involved in acute cardiac dysfunction in patients with dystrophinopathy because vaccination or inhibitors of the coxsackieviral protease 2A could be available.[26]

Despite the same exonic deletion, patients 1 and 2 showed juvenile-onset heart failure without overt skeletal myopathy, while patient 3 revealed a late-onset BMD phenotype with only slight cardiac dysfunction. It is therefore intriguing to consider what factors contributed to these phenotypic differences. One possible genetic factor is a cardio-specific cis-element present in intron 44 or intron 55 that is missing from patients 1 and 2, but not from patient 3. To investigate whether the deleted region in each intron was different in these three patients, we attempted to amplify the intronic junctional fragment by long-PCR. Unfortunately this approach failed, probably because the intact region of intron 44 and/or 55 is too large for PCR amplification.

In general, XLDCM patients having mutations in the 5' end of the *DMD* gene have a very poor prognosis.[2,3,6] However, the XLDCM phenotype coinciding with deletion of exons 45–55 may be associated with long-term survival if cardiac care is properly managed. Interestingly, it has been reported that an in-frame deletion including the hinge III region, which is encoded by exons 50 and 51, results in milder phenotypes as compared with shorter deletions that do not include the hinge III region.[22] The hinge III region is disrupted in our patients, and their phenotype is roughly comparable with that report. However, any association with cardiac involvement is not known. Further investigation will be needed to understand the relationship between genotype and cardiac phenotype in the distal rod domain, including the hinge region.

Acknowledgement

This work was supported by a Research Grant for Nervous and Mental Disorders (8A-2) from the Ministry of Health and Welfare. Anti-dystrophin antibody MANEX1A was provided by Dr. GE Morris, Multi-Disciplinary Research and Innovation Centre Biochemistry Group, The North East Wales Institute.

References

1. Berko BA, Swift M. X-linked dilated cardiomyopathy. *N Engl J Med* 1987;**316**:1186–91.
2. Towbin JA, Hejtmancik JF, Brink P, et al. X-linked dilated cardiomyopathy. Molecular genetic evidence of linkage to the Duchenne muscular dystrophy (dystrophin) gene at the Xp21 locus. *Circulation* 1993;**87**:1854–65.
3. Muntoni F, Cau M, Ganau A, et al. Deletion of the dystrophin muscle-promoter region associated with X-linked dilated cardiomyopathy. *N Engl J Med* 1993;**329**:921–5.
4. Milasin J, Muntoni F, Severini GM, et al. A point mutation in the 5' splice site of the dystrophin gene first intron responsible for X-linked dilated cardiomyopathy. *Hum Mol Genet* 1996;**5**:73–9.
5. Bies RD, Maeda M, Roberds SL, et al. A 5' dystrophin duplication mutation causes membrane deficiency of alpha-dystroglycan in a family with X-linked cardiomyopathy. *J Mol Cell Cardiol* 1997;**29**:3175–88.
6. Yoshida K, Nakamura A, Yazaki M, et al. Insertional mutation by transposable element, L1, in the DMD gene results in X-linked dilated cardiomyopathy. *Hum Mol Genet* 1998;**7**:1129–32.
7. Muntoni F, Di Lenarda A, Porcu M, et al. Dystrophin gene abnormalities in two patients with idiopathic dilated cardiomyopathy. *Heart* 1997;**78**:608–12.
8. Arbustini E, Diegoli M, Morbini P, et al. Prevalence and characteristics of dystrophin defects in adult male patients with dilated cardiomyopathy. *J Am Coll Cardiol* 2000;**35**:1760–8.
9. Ortiz-Lopez R, Li H, Su J, et al. Evidence for a dystrophin missense mutation as a cause of X-linked dilated cardiomyopathy. *Circulation* 1997;**95**:2434–40.
10. Ferlini A, Galie N, Merlini L, et al. A novel Alu-like element rearranged in the dystrophin gene causes a splicing mutation in a family with X-linked dilated cardiomyopathy. *Am J Hum Genet* 1998;**63**:436–46.
11. Franz WM, Muller M, et al. Association of nonsense mutation of dystrophin gene with disruption of sarcoglycan complex in X-linked dilated cardiomyopathy. *Lancet* 2000;**355**:1781–5.
12. Ferlini A, Sewry C, Melis MA, et al. X-linked dilated cardiomyopathy and the dystrophin gene. *Neuromuscl Disord* 1999;**9**:339–46.
13. Muntoni F, Melis MA, Ganau A, et al. Transcription of the dystrophin gene in normal tissues and in skeletal muscle of a family with X-linked dilated cardiomyopathy. *Am J Hum Genet* 1995;**56**:151–7.
14. Muntoni F, Wilson L, Marrosu G, et al. A mutation in the dystrophin gene selectively affecting dystrophin expression in the heart. *J Clin Invest* 1995;**96**:693–9.
15. Nakamura A, Ikeda S, Yazaki M, et al. Up-regulation of the brain and Purkinje-cell forms of dystrophin transcripts, in Becker muscular dystrophy. *Am J Hum Genet* 1997;**60**:1555–8.
16. Piccolo G, Azan G, Tonin P, et al. Dilated cardiomyopathy requiring cardiac transplantation as initial manifestation of Xp21 Becker type muscular dystrophy. *Neuromuscl Disord* 1994;**4**:143–6.
17. Siciliano G, Fanin M, Angelini C, et al. Prevalent cardiac involvement in dystrophin Becker type mutation. *Neuromuscl Disord* 1994;**4**:381–6.
18. Muntoni F, Torelli S, Ferlini A. Dystrophin and mutations: one gene, several proteins, multiple phenotypes. *Lancet Neurol* 2003;**2**:731–40.
19. Beggs AH, Hoffman EP, Snyder JR, et al. Exploring the molecular basis for variability among patients with Becker muscular dystrophy: dystrophin gene and protein studies. *Am J Hum Genet* 1991;**49**:54–67.

20. Tasaki N, Yoshida K, Haruta S, et al. X-linked dilated cardiomyopathy with a large hot-spot deletion in the dystrophin gene. *Intern Med* 2001;**40**:1215–21.
21. Yazaki M, Yoshida K, Nakamura A, et al. Clinical characteristics of aged Becker muscular dystrophy patients with onset after 30 years. *Eur Neurol* 1999;**42**:145–9.
22. Carsana A, Frisso G, Tremolaterra MR, et al. Analysis of dystrophin gene deletions indicates that the hinge III region of the protein correlates with dsease severity. *Ann Human Genet* 2005;**69**:253–9.
23. Ishikawa Y, Bach JR, Minami R. Cardioprotection for Duchenne's muscular dystrophy. *Am Heart J* 1999;**137**:895–902.
24. Jefferies JL, Eidem BW, Belmont JW, et al. Genetic predictors and remodeling of dilated cardiomyopathy in muscular dystrophy. *Circulation* 2005;**112**:2799–804.
25. Xiong D, Lee GH, Badorff C, et al. Dystrophin deficiency markedly increases enterovirus-induced cardiomyopathy: a genetic predisposition to viral heart disease. *Nat Med* 2002;**8**: 872–7.
26. Badorff C, Fichtlscherer B, Rhoads RE, et al. Nitric oxide inhibits dystrophin proteolysis by coxsackieviral protease 2A through S-nitrosylation: A protective mechanism against enteroviral cardiomyopathy. *Circulation* 2000;**102**:2276–81.

Selective Vacuolar Degeneration in Dystrophin-Deficient Canine Purkinje Fibers Despite Preservation of Dystrophin-Associated Proteins With Overexpression of Dp71

Nobuyuki Urasawa, MD; Michiko R. Wada, PhD; Noboru Machida, DVM, PhD; Katsutoshi Yuasa, PhD; Yoshiki Shimatsu, PhD; Yoshito Wakao, DVM, PhD; Shigeki Yuasa, MD, PhD; Toshiaki Sano, MD, PhD; Ikuya Nonaka, MD, PhD; Akinori Nakamura, MD, PhD; Shin'ichi Takeda, MD, PhD

Background—Respiratory support therapy significantly improves life span in patients with Duchenne muscular dystrophy; cardiac-related fatalities, including lethal arrhythmias, then become a crucial issue. It is therefore important to more thoroughly understand cardiac involvement, especially pathology of the conduction system, in the larger Duchenne muscular dystrophy animal models such as dystrophic dogs.

Methods and Results—When 10 dogs with canine X-linked muscular dystrophy in Japan ($CXMD_J$) were examined at the age of 1 to 13 months, dystrophic changes of the ventricular myocardium were not evident; however, Purkinje fibers showed remarkable vacuolar degeneration as early as 4 months of age. The degeneration of $CXMD_J$ Purkinje fibers was coincident with overexpression of Dp71 at the sarcolemma and translocation of μ-calpain to the cell periphery near the sarcolemma or in the vacuoles. Immunoblotting of the microdissected fraction showed that μ-calpain–sensitive proteins such as desmin and cardiac troponin-I or -T were selectively degraded in the $CXMD_J$ Purkinje fibers. Utrophin was highly upregulated in the earlier stage of $CXMD_J$ Purkinje fibers, but the expression was dislocated when vacuolar degeneration was recognized at 4 months of age. Nevertheless, the expression of dystrophin-associated proteins α-, β-, γ-, and δ-sarcoglycans and β-dystroglycan was well maintained at the sarcolemma of Purkinje fibers.

Conclusions—Selective vacuolar degeneration of Purkinje fibers was found in the early stages of dystrophin deficiency. Dislocation of utrophin besides upregulation of Dp71 can be involved with this pathology. The degeneration of Purkinje fibers can be associated with the distinct deep Q waves in ECG and fatal arrhythmia seen in dystrophin deficiency. (***Circulation.*** **2008;117:2437-2448.)**

Key Words: cardiomyopathy ■ conduction ■ dystrophin ■ Purkinje fibers ■ utrophin

Duchenne muscular dystrophy (DMD) is a lethal X-linked disorder caused by mutations in the *DMD* gene.[1] Seven promoters in the huge *DMD* gene drive tissue-specific expression of 427-kDa full-length dystrophins and various C-terminal isoforms such as Dp71.[2] The full-length muscle-type dystrophin is located at the inner surface of the sarcolemma with dystrophin-associated proteins (DAPs) and forms the dystrophin-glycoprotein complex linking the intracellular actin cytoskeleton of myofibers to the extracellular matrix.[3] A lack of dystrophin prevents the assembly of DAPs on the sarcolemma and leads to muscle degeneration. Utrophin, an autosomal homologue of dystrophin, is upregulated in dystrophin-deficient muscles of DMD and the animal models.[4] It has been considered that utrophin overexpression at the sarcolemma compensates for the lack of dystrophin in dystrophic muscle.[4,5]

Clinical Perspective p 2448

In humans, the loss of dystrophin accompanied by a deficiency of dystrophin-glycoprotein complex at the sarcolemma leads to progressive degeneration not only in skeletal muscle but also in cardiac muscle. The subsequent respiratory or cardiac failure causes death at an early age, but recent progress in the use of respirators has reduced the rate of death due to respiratory failure and improved the prognosis. Consequently, cardiac death has become a serious problem. The cardiac involvement in DMD is characterized by cardiomyopathy, cardiac arrhythmias, and distinctive ECG findings.

Received September 9, 2007; accepted March 5, 2008.

From the Departments of Molecular Therapy (N.U., M.R.W., K.Y., Y.S., A.N., S.T.) and Ultrastructural Research (S.Y.), National Institute of Neuroscience, National Center of Neurology and Psychiatry, Kodaira, Tokyo, Japan; Department of Veterinary Pathology, Tokyo University of Agriculture and Technology, Fuchu, Tokyo, Japan (N.M.); Department of Veterinary Surgery I, Azabu University, Sagamihara, Kanagawa, Japan (Y.W.); Department of Pathology, University of Tokushima Graduate School of Medicine, Tokushima, Japan (T.S.); and National Hospital for Mental, Nervous, and Muscular Disorders, National Center of Neurology and Psychiatry, Kodaira, Tokyo, Japan (I.N.).

Correspondence to Shin'ichi Takeda, MD, PhD, Department of Molecular Therapy, National Institute of Neuroscience, National Center of Neurology and Psychiatry, 4-1-1 Ogawa-higashi, Kodaira, Tokyo 187-8502, Japan. E-mail takeda@ncnp.go.jp

Circulation is available at http://circ.ahajournals.org

DOI: 10.1161/CIRCULATIONAHA.107.739326

Progressive myocardial fibrosis primarily in the posterobasal region of the left ventricle (LV) results in dilated cardiomyopathy.[6] Various arrhythmias such as ventricular tachycardia, atrioventricular block, bundle-branch block, and fascicular block are often observed in DMD.[7–9] In DMD patients, the prevalence of lethal arrhythmias has been considered to be lower than that in myotonic dystrophy or Emery-Dreifuss muscular dystrophy, but some studies showed that sudden death accounts for 12.1% of all deaths of DMD patients and that ventricular arrhythmia is an important cause of death.[8] A distinctive ECG pattern of deep narrow Q waves in leads I, aVL, and V_5 through V_6 or II, III, and aVF has been detected and is ascribed to myocardial fibrosis in the posterobasal region of the LV.[6]

The X-chromosome–linked muscular dystrophy (*mdx*) mouse and the golden retriever muscular dystrophy dog (GRMD) lack dystrophin and serve as models for DMD. The phenotypic expression of GRMD is more similar to DMD than that of the *mdx* mouse,[10] and GRMD shows progressive cardiomyopathy and deep, narrow Q waves in leads II, III, and aVF comparable to cardiac involvement in human subjects.[10,11] However, it is very difficult to maintain a GRMD colony because of their severe phenotypes. On the other hand, interbreeding of GRMD with small dogs results in mild phenotypes of the disease.[10] Thus, we have developed a beagle-based colony of medium-sized dogs and named it canine X-linked muscular dystrophy in Japan ($CXMD_J$).[12] Beagle-based dystrophic dogs show mild phenotypes not only in skeletal muscle[13] but also in cardiac muscle.[14] Moreover, we found that the distinctive deep Q waves precede the LV posterobasal lesion on echocardiography and histopathology in $CXMD_J$.[14] The histopathological changes in the conduction system have not been investigated fully, especially in the early stages of the disease, although the expressions of dystrophin and DAPs have been examined in normal systems.[15–18]

The molecular mechanisms of the dystrophin-deficient heart are still unclear. Two main possibilities exist relative to the functional roles of dystrophin. One hypothesis is that dystrophin maintains the structural integrity of the sarcolemma and confers mechanical strength during muscle contraction.[19] The membrane tears due to dystrophin deficiency may increase the permeability to Ca^{2+}, which might trigger protease activity.[20] The second hypothesis is proposed because dystrophin and DAPs anchored neuronal nitric oxide synthase, aquaporin-4, and Na^+ channel at the sarcolemma, and L-type Ca^{2+} channels and stretch-activated channels were also regulated by expression of dystrophin and DAPs. The expression and functions of these membrane-associated proteins were altered in the absence of dystrophin, which may lead to dysfunction of muscle fibers.[21] Either stretch-activated channels[21] or the enhancement of the open probability of leak channels[22] was involved in dystrophin-deficient muscle, resulting in elevation of the Ca^{2+} influx. Elevated $[Ca^{2+}]_i$ acts on the autoproteolysis cascade, leading to myofilament destruction and/or muscle cell death by activation of calcium-dependent cysteine proteases, the calpains.[23,24] The main isoforms of the calpain family, m- and μ-calpain, are activated in vitro in the presence of millimolar and micromolar concentrations of Ca^{2+}, respectively. In dystrophin-deficient skeletal muscle, calpains are increased and activated at the pathological stage.[24]

In this study, we examined the conduction system in the $CXMD_J$ heart. We show here for the first time that dystrophin deficiency results in selective degeneration of Purkinje fibers. Furthermore, activation of μ-calpain and dislocation of utrophin with Dp71 overexpression were observed in the early stage of $CXMD_J$ Purkinje fibers.

Methods

Animals

We determined the serum creatine kinase levels and genotypes of $CXMD_J$ and normal littermate pups soon after birth. Moreover, we routinely examined the dogs for clinical manifestations including gait and mobility disturbances, involvement of limb, temporal and tongue muscles, dysphagia, and drooling according to our clinical grading scale.[13] In this study, we used third-generation $CXMD_J$ dogs (n=10) and normal third-generation dogs (n=7) from 1 to 13 months of age, but we mainly examined 4 $CXMD_J$ and 2 normal littermate dogs at 4 months of age and a pair of $CXMD_J$ and normal littermate dogs at 1 and 2 months of age in the time course analysis because the number of $CXMD_J$ dogs available is limited. The phenotype of these affected dogs has been described previously.[13,14] All experimental animals were part of the $CXMD_J$ breeding colony at the General Animal Research Facility, National Institute of Neuroscience, National Center of Neurology and Psychiatry (Tokyo, Japan)[12] or the Chugai Research Institute for Medical Science, Inc (Nagano, Japan). The dogs were cared for and treated in accordance with the guidelines provided by the Ethics Committee for the Treatment of Laboratory Animals of the National Institute of Neuroscience or the Ethics Committee for Treatment of Laboratory Animal of Chugai Pharmaceutical Co, Ltd (Tokyo, Japan). These studies were also approved by the Ethics Committee for the Treatment of Laboratory Middle-Sized Animals of the National Institute of Neuroscience (approval Nos. 13-03, 14-03, 15-03, 16-03, 17-03, and 18-03). Skilled experimental animal technologists, who have special knowledge of methods to prevent unnecessary excessive pain, handled the dogs and assisted in the experiments.

Light Microscopy

Pathological changes in the heart were analyzed within 1 week of the performance of ECG and echocardiography. After a dog was given an overdose of intravenous pentobarbital, the whole heart was removed. To prepare specimens for immunologic analysis and electron microscopy, the block of the endocardial sides containing Purkinje fibers was dissected out from the interventricular septum and anterior, posterior, and lateral walls of the LV at the level of papillary muscles. The remaining heart was immediately fixed in 15% buffered formalin for histological analysis. Formalin-fixed hearts were dissected into separate blocks containing ventricular myocardium and/or conduction systems, ie, the sinus node, atrioventricular node, bundle of His, left and right bundle branches, and Purkinje fibers from the LV or right atrium, as described elsewhere.[25] Each piece of tissue was embedded in paraffin, and 10-μm sections were stained with hematoxylin and eosin. Photographs were taken with a DAS Mikroskop Leits DMRB microscope (Leica, Wetzlar, Germany) with the use of a digital still camera system HC-2500 (Fujifilm, Tokyo, Japan).

Electron Microscopy

Muscles from the LV were fixed in 2% glutaraldehyde, postfixed in osmium tetroxide, dehydrated in a graded ethanol series, and then embedded in Epon. Ultrathin sections stained with uranyl acetate and lead citrate were examined by H-7000 transmission electron microscopy (Hitachi High Technologies, Tokyo, Japan).

Immunohistochemistry

Seven-micrometer transverse cryosections of frozen LV muscles were fixed in acetone, blocked with 5% goat serum, and incubated with mouse monoclonal antibodies against various epitopes of dystrophin: MANEX1a recognizing amino acids 3 to 10 of muscle-type dystrophin molecule (generous gift of Dr G.E. Morris, Wolfson Centre for Inherited Neuromuscular Disease),[26] NCL-DYSB recognizing amino acids 321 to 494 (Novocastra Laboratories, Newcastle, UK), NCL-DYS1 recognizing amino acids 1181 to 1388 (Novocastra), MANDYS8 recognizing amino acids 1431 to 1505 (Sigma-Aldrich, St Louis, Mo), F22.9C5 recognizing amino acids 1840 to 2266 (Alexis, Lausen, Switzerland), or NCL-DYS2 recognizing amino acids 3669 to 3685 (Novocastra); mouse monoclonal antibodies against β-dystroglycan (NCL-b-DG, Novocastra), β-sarcoglycan (NCL-b-SG, Novocastra), γ-sarcoglycan (NCL-g-SG, Novocastra), or δ-sarcoglycan (DSG-1)[27]; rabbit polyclonal antibodies against utrophin (UT-2),[28] α-sarcoglycan (α-SG2),[29] or μ-calpain (anti-calpain I large subunit domain IV; Sigma-Aldrich). The primary antibodies were labeled with fluorescein-conjugated goat anti-mouse or anti-rabbit immunoglobulin G (Molecular Probes, Eugene, Ore), and signals were recorded photographically with a confocal laser scanning microscope (TCSSP, Leica).

Immunoblot Analysis

For immunoblot analysis of ventricular myocardium or Purkinje fibers, laser capture microdissection was performed with the use of an LM 200 system (Arcturus, Mountain View, Calif), as described elsewhere with some modifications.[30] Fifteen-micrometer cryosections were prepared from frozen LV muscles and dehydrated in graded ethanols and xylene. Eight hundred 15-μm diameter microdissection spots were collected from ventricular myocardium or Purkinje fibers onto each CapSure Macro LCM Cap (Arcturus). Tissues captured on Caps were suspended in 20 μL of SDS-PAGE lysis buffer (10% SDS, 70 mmol/L Tris-HCl, pH 6.8, 5% β-mercaptoethanol, 10 mmol/L EDTA) at 80°C for 15 minutes. Ten-microliter aliquots were separated in each lane on 7.5% or 9% SDS-PAGE and electrotransferred onto a polyvinylidene fluoride membrane (Immobilon; Millipore, Billerica, Mass), as previously described.[28,29,31] Equality of the protein concentrations was confirmed by Coomassie blue staining, and myosin heavy chain was used as the loading control. After blocking by 2% casein in Tris-buffered saline, the blot was incubated with mouse monoclonal antibody against dystrophin (NCL-DYS2, which recognizes amino acids 3669 to 3685 corresponding to exon 78), rabbit polyclonal antibody against dystrophin (anti-Ex71, which recognizes amino acids 3406 to 3425 corresponding to exon 71, or p34a, which recognizes amino acids 3495 to 3544 corresponding to exon 75, a generous gift of Dr M. Yoshida, National Institute of Neuroscience),[31,32] utrophin (UT-2), α-sarcoglycan (α-SG2), μ-calpain (anti-calpain I large subunit domain IV), desmin (Progen, Heidelberg, Germany), cardiac troponin-T (6G9; HyTest, Turku, Finland), cardiac troponin-I (16A11; RDI division of Fitzgerald Industries International, Concord, Mass), and α-sarcomeric actin, which was used as an internal control (EA-53; Sigma-Aldrich). Primary antibodies were detected by horseradish peroxidase–conjugated goat anti-mouse immunoglobulin G (Bio-Rad, Hercules, Calif) or anti-rabbit immunoglobulin G (Jackson Laboratory, Bar Harbor, Me) and ECL Plus Western blotting detection reagents (Amersham Biosciences, Uppsala, Sweden).

The authors had full access to and take full responsibility for the integrity of the data. All authors have read and agree to the manuscript as written.

Results

Selective Degeneration of Purkinje Fibers in $CXMD_J$

We investigated morphological abnormalities in the cardiac conduction system of $CXMD_J$. In all $CXMD_J$ dogs, the sinus node, atrioventricular node, and bundle of His showed no degenerative changes (Figure 1A). Many irregular vacuoles were observed, but only in Purkinje fibers (Figure 1A and 1B). Remarkable vacuolar degeneration was consistently observed in $CXMD_J$ Purkinje fibers in dogs at 4 months old (Figure 1C), whereas degeneration and fibrosis were absent in the ventricular myocardium (Table). These results imply that Purkinje fibers are susceptible to dystrophin deficiency, which causes selective and progressive vacuolar degeneration in an early stage of the disease.

Using transmission electron microscopy, we examined the contents of the vacuoles of $CXMD_J$ Purkinje fibers. On electron microscopy, almost all myofibrils and intracellular organelles had disappeared, and disrupted myofibrils and fragmented mitochondria were observed in the vicinity of the vacuoles (Figure 2). These results suggest that the vacuoles are the ruins of myofibrillar structures. In $CXMD_J$ ventricular myocardium, which seemed healthy on the light microscopic level, mildly disrupted myofibrils and mitochondrial fragmentation were observed on electron microscopy (Figure 2).

Upregulation of Dystrophin Short-Isoform Dp71 in $CXMD_J$ Purkinje Fibers

The causative mutation of $CXMD_J$ is located in the 3′ splice site of intron 6 in the canine dystrophin gene.[33] Thus, we examined whether the truncated C-terminal dystrophin isoforms were expressed in the Purkinje fibers. In control dogs, the sarcolemma of ventricular cardiomyocytes and Purkinje fibers was stained with all the anti-dystrophin antibodies used in this study: MANEX1a, NCL-DYSB, F22.9C5, NCL-DYS2 (Figure 3A), NCL-DYS1, and MANDYS8 (data not shown). The ventricular myocardium of $CXMD_J$ lacked expression of the full-length dystrophin and its short isoforms, but the sarcolemma of $CXMD_J$ Purkinje fibers was clearly stained with NCL-DYS2, which recognizes the C-terminal of full-length dystrophin and its isoforms (Figure 3A).

To confirm which dystrophin isoform is present in the Purkinje fibers, we selectively collected Purkinje fibers using laser capture microdissection. The result showed thick doublet bands around 71 to 75 kDa in $CXMD_J$ Purkinje fibers and thin doublet bands in normal Purkinje fibers stained with NCL-DYS2 antibody (Figure 3B). These data suggest that the sarcolemma of $CXMD_J$ Purkinje fibers lacked full-length dystrophin but showed overexpression of a C-terminal isoform of dystrophin, Dp71. Dp71 is well known to cause alternative splicing in exon 71 and/or exon 78. Therefore, we used several anti-dystrophin C-terminal antibodies that can recognize the various epitopes corresponding to exon 71, exon 75, and exon 78 (anti-Ex71, p34a, and NCL-DYS2, respectively) and performed immunoblot analyses. Each antibody revealed doublet bands (Figure 3C); therefore, the doublet bands were not the result of alternative splicing in exon 71 and/or exon 78. Dp71 was also reported to be detected as doublet, with the upper band being phosphorylated.[34,35] Therefore, the upper band in Purkinje fibers of normal and $CXMD_J$ dogs can be phosphorylated Dp71.

Expression of Utrophin and Preservation of DAPs in $CXMD_J$ Purkinje Fibers

We found that the expression of Dp71 is certainly increased in $CXMD_J$ Purkinje fibers. In the dystrophin-deficient mus-

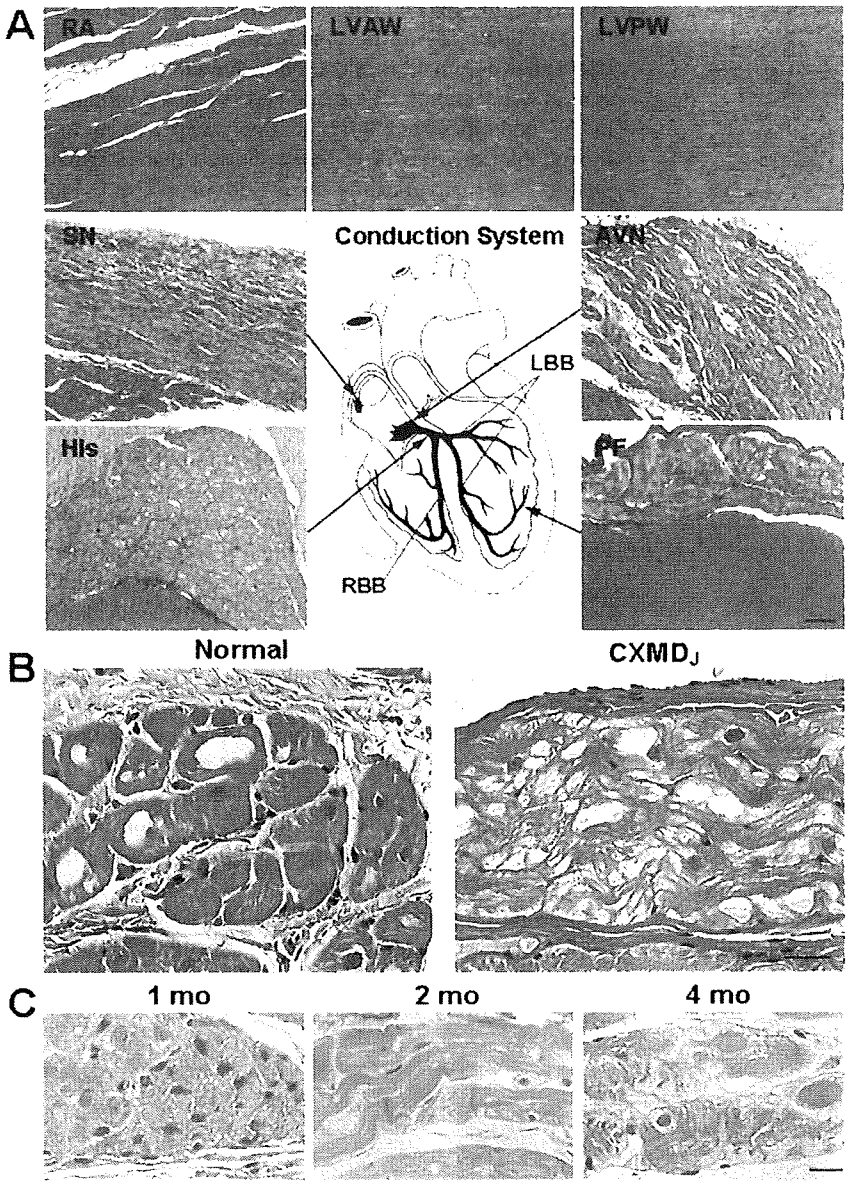

Figure 1. Histopathology of hearts of CXMD$_J$ dogs. A, Hematoxylin and eosin–stained sections from the heart of a 13-month-old affected dog (III-D12MA in the Table) show representative histopathological findings in hearts of CXMD$_J$. RA indicates right atrium; LVAW, LV anterior wall; LVPW, LV posterior wall; SN, sinus node; AVN, atrioventricular node; His, bundle of His; and PF, Purkinje fibers. Bar=100 μm. The conduction system is illustrated in the center. LBB indicates left bundle branches; RBB, right bundle branches. B, Purkinje fibers from a normal 12-month-old dog (III-D23MN in the Table) and the affected dog shown in A. Bar=25 μm. C, Purkinje fibers from 1-, 2-, and 4-month-old affected dogs (III-203 MA, III-202MA, and III-E02MA, respectively, in the Table). Bar=25 μm.

cle, utrophin, an autosomal homologue of dystrophin, is compensatorily upregulated.[4,5] We therefore investigated the expression of utrophin to assess the effect of overexpression of Dp71 at the sarcolemma in CXMD$_J$ Purkinje fibers. In control dogs, utrophin was present in intercalated disks and small vessels in the ventricular myocardium and also weakly expressed at the sarcolemma of Purkinje fibers (Figure 4A). In CXMD$_J$, utrophin was present at the sarcolemma of ventricular cardiomyocytes, and, very interestingly, utrophin was upregulated in Purkinje fibers (Figure 4A). Immunoblot analysis also showed that utrophin was increased in the CXMD$_J$ Purkinje fibers when examined at 4 months of age (Figure 4B), although we further evaluated utrophin expression along with the time in subsequent sections.

Reduction of all of the DAPs has been reported in dystrophin-deficient muscle.[3] We also examined distribution of the DAPs β-dystroglycan and α-, β-, γ-, and δ-sarcoglycans in CXMD$_J$ Purkinje fibers. In CXMD$_J$, expression of α-sarcoglycan was well maintained in Purkinje fibers but reduced in the ventricular myocardium (Figure 4A). The same tendency was observed in other DAP expressions (data not shown). The immunoblot analysis showed that the expression level of α-sarcoglycan was preserved in the microdissected CXMD$_J$ Purkinje fibers but not in the CXMD$_J$ myocardium (Figure 4B).

Activation and Accumulation of μ-Calpain in CXMD$_J$ Purkinje Fibers

Upregulated utrophin and well-maintained DAPs do not guarantee the integrity of the sarcolemma in dystrophin-deficient Purkinje fibers. We asked why the myofibrils were severely disrupted in the CXMD$_J$ Purkinje fibers. One hypothesis was that an alteration of expression or function of several membrane-associated molecules such as Ca^{2+} channels results in activation of 1 or more calcium-dependent proteases such as μ-calpain.[21–24] We therefore investigated

Table. Evaluation of Histopathological Changes in the Heart

Dog No.	Age, mo	Fibrosis of LV Wall	Degeneration of Purkinje Fibers
$CXMD_J$			
III-203MA	1	–	–
III-202MA	2	–	–/+
III-E02MA	4	–	+
III-E07MA	4	–	++
III-E08MA	4	–	+++
III-1903MA	4	–	+++
III-D33MA	6	–	+++
III-D53MA	6	–	++
III-D55MA	9	–	+++
III-D12MA	13	–	+++
Control			
III-204MN	1	–	–
III-E09MN	2	–	–
III-2006FN	3	–	–
III-403MN	4	–	–
III-E01MN	4	–	–
III-D56MN	6	–	–
III-D23MN	12	–	–

The extent of histopathological changes of the heart is shown as –, none or within normal range; –/+, minimal; +, mild; ++, moderate; and +++, severe.

the expression of μ-calpain in $CXMD_J$ Purkinje fibers. Immunohistochemical analysis showed that the expression of μ-calpain was accumulated only in $CXMD_J$ Purkinje fibers (Figure 5A). Furthermore, μ-calpain localized at the cell periphery near the sarcolemma in nonvacuolated Purkinje fibers (Figure 5A) and at the vacuoles in vacuolated Purkinje fibers (Figure 5B) in the same $CXMD_J$ heart. These results imply that μ-calpain localization is altered with the progression of degeneration. We examined μ-calpain protein levels in the microdissected Purkinje fibers and myocardium by immunoblot analysis. The result showed that μ-calpain expression was significantly increased in $CXMD_J$ Purkinje fibers but not in $CXMD_J$ ventricular myocardium at 4 months of age (Figure 5C).

Time Course of Dp71 Expression, μ-Calpain Translocation, and Utrophin Expression in $CXMD_J$ Purkinje Fibers

We next investigated the time course of expressions of Dp71, μ-calpain, and utrophin in 1-, 2-, and 4-month-old $CXMD_J$ dogs to understand the relationship among them. In immunohistochemical and immunoblot analyses, the expression of Dp71 was clearly increased in 4-month-old $CXMD_J$ Purkinje fibers (Figure 6A and 6B). Similarly, the subsarcolemmal accumulation of μ-calpain was also observed in 4-month-old $CXMD_J$ Purkinje fibers in the immunohistochemical analysis (Figure 6A), but the concentration of μ-calpain was not changed in the immunoblot analysis (Figure 6B). These data indicate the subsarcolemmal translocation of μ-calpain. The degeneration of $CXMD_J$ Purkinje fibers was consistently observed at the age of 4 months, as described (Figure 1C). Therefore, overexpression of Dp71 and translocation of μ-calpain may be involved in the degeneration of $CXMD_J$ Purkinje fibers. In turn, utrophin expression was gradually reduced with time in both normal and $CXMD_J$ ventricular myocardium (Figure 6A and 6C), but the reduction was more evident in $CXMD_J$ Purkinje fibers (Figure 6C). The sharp reduction of utrophin might be related to upregulation of Dp71 in $CXMD_J$ Purkinje fibers at this period.

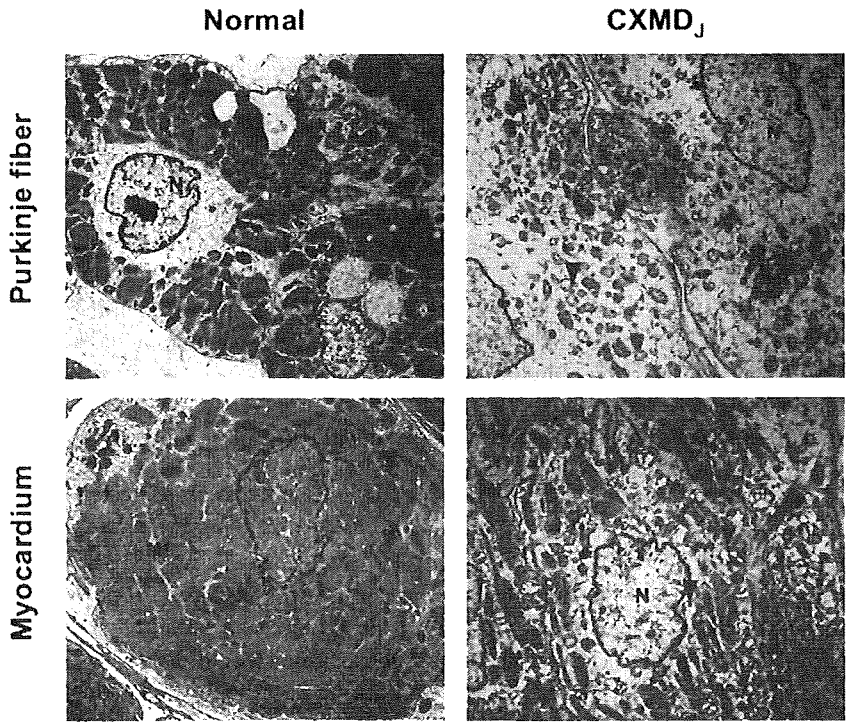

Figure 2. Ultrastructure of Purkinje fibers (top panels) and ventricular myocardium (bottom panels) from normal (III-403MN in the Table) and affected (III-E07MA in the Table) 4-month-old dogs. N indicates nucleus; Mf, myofibril. Arrowheads indicate mitochondria. Bar=1 μm.

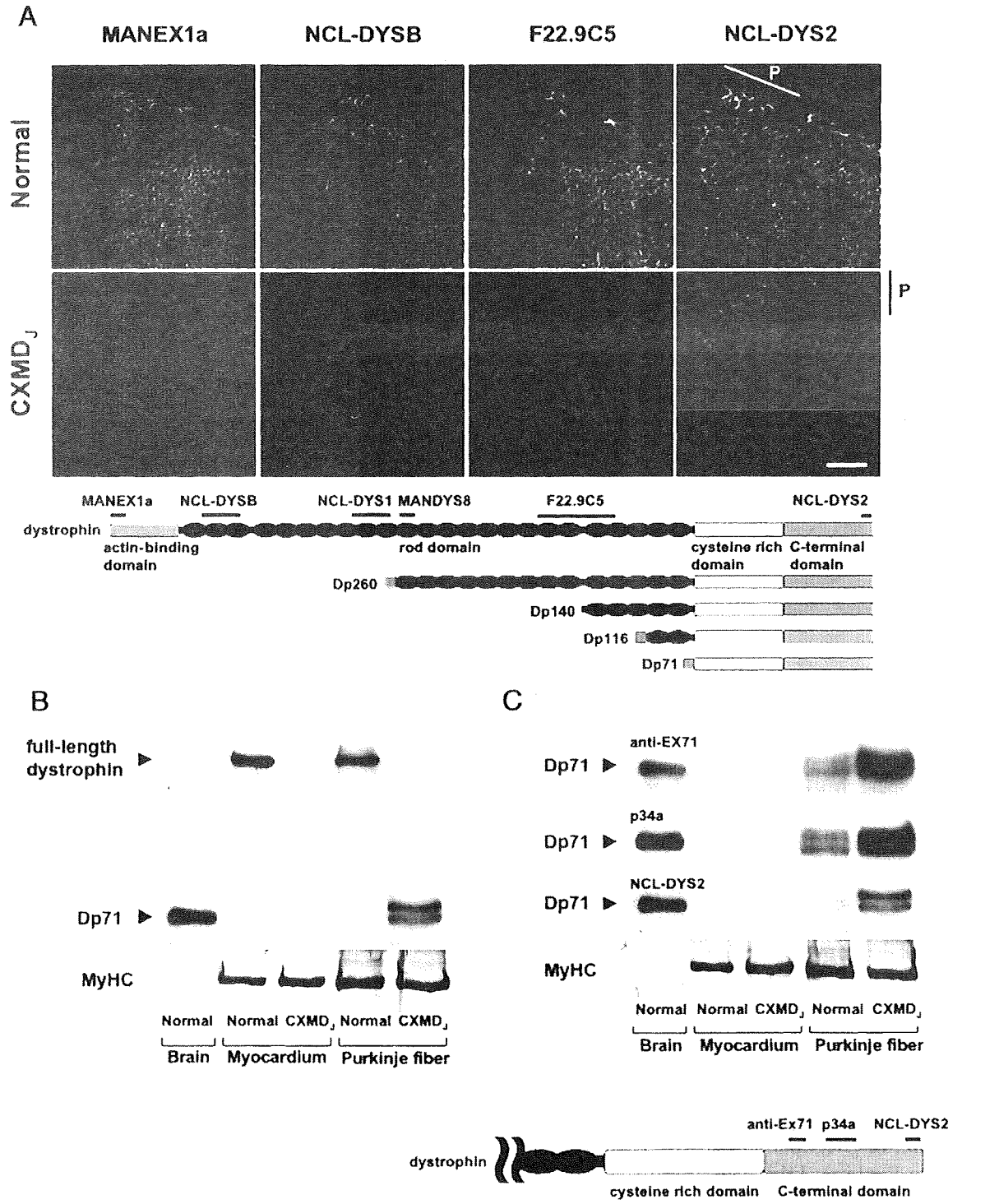

Figure 3. Expression of dystrophin and dystrophin C-terminal isoforms in LV of normal and CXMD$_J$ dogs. A, Immunohistochemical staining using several anti-dystrophin antibodies of the LV of normal (III-E01MN in the Table) and affected (III-E02MA in the Table) 4-month-old dogs. Serial cryosections from the LV were stained with MANEX1a, NCL-DYSB, F22.9C5, and NCL-DYS2 antibodies, which recognize different epitopes of dystrophin (see Methods and schema). P indicates Purkinje fibers. Bar = 100 μm. The bottom schema shows full-length dystrophin and C-terminal short isoforms with the positions of epitopes recognized by each anti-dystrophin antibody (bars). B, Immunoblot analysis using the anti-dystrophin C-terminal antibody NCL-DYS2. Samples from the dogs shown in A were separated by SDS-PAGE on 9% acrylamide gel. Extracts from affected Purkinje fibers showed thick doublet bands around 71 to 75 kDa. Those bands could be Dp71 with the upper band being phosphorylated. Myosin heavy chain (MyHC) was used as the loading control. C, Immunoblot analyses of the samples described in B using the anti-dystrophin C-terminal antibodies anti-Ex71, p34a, and NCL-DYS2. Myosin heavy chain was used as the loading control. Each antibody recognizes a different epitope on the dystrophin C-terminal (see Methods and schema). Extracts from affected Purkinje fibers reacted with all antibodies around 71 to 75 kDa. The bottom schema shows the positions of dystrophin C-terminal epitopes recognized by each anti-dystrophin C-terminal antibody (bars).